

AD-A113 254

HUGHES AIRCRAFT CO .TORRANCE CA ELECTRON DYNAMICS DIV

F/G 9/1

MULTIMODE AMPLIFIER.(U)

FEB 82 A L ROUSSEAU, I TAMMARU

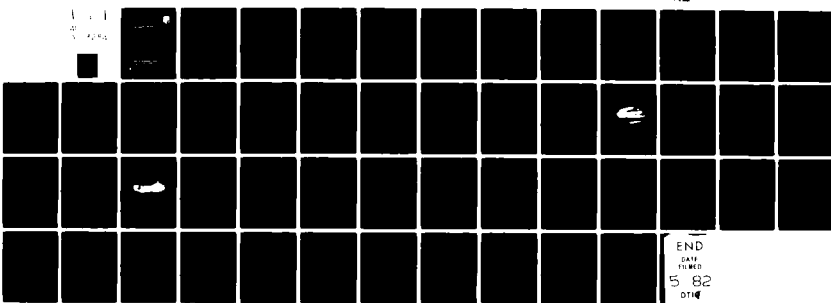
F30602-79-C-0002

UNCLASSIFIED

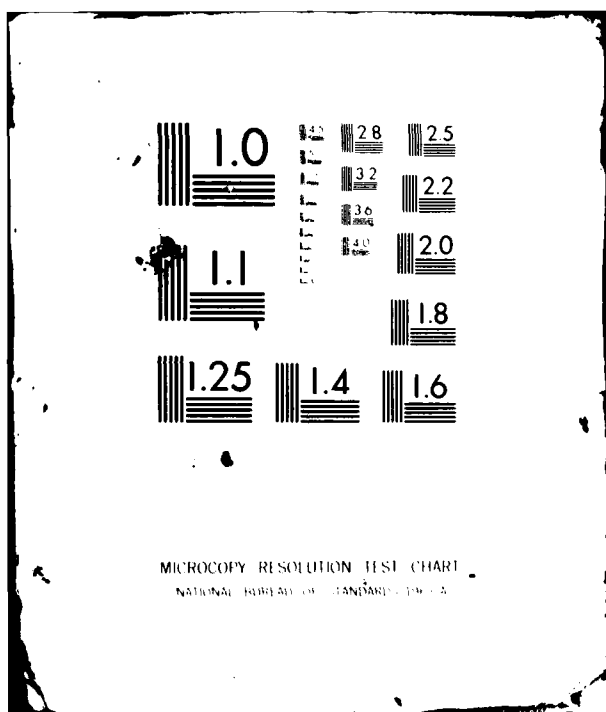
HAC-W-08193

RADC-TR-82-4

NL



END  
DATE  
FORMED  
5-82  
DTIG



AD A113254

## MULTIMODE AMPLIFIER

HOHNER AIRCRAFT COMPANY

Anthony L. Rauschow  
Manager

APPROVED FOR PUBLIC RELEASE. DISTRIBUTION UNLIMITED

NEW YORK AIR NATIONAL GUARD  
Air Force Systems Command  
Queens Air Force Base, New York 11428

32-98

SDTIC  
ELECTRIC  
MAY 3 1982

THE BOSTONIAN

Johnson 3 - 1968-1969  
Project Executive

卷之三

## FOR THE COMMANDER

*John G. Miller*  
John G. Miller  
10000 7th Street  
Los Angeles, California

卷之三

## UNCLASSIFIED

SECURITY CLASSIFICATION OF THIS PAGE (When Data Entered)

REPORT DOCUMENTATION PAGE		READ INSTRUCTIONS BEFORE COMPLETING FORM
1. REPORT NUMBER RADC-TR-82-4	2. GOVT ACCESSION NO. 42 4113 254	3. RECIPIENT'S CATALOG NUMBER
4. TITLE (and Subtitle) MULTIMODE AMPLIFIER	5. TYPE OF REPORT & PERIOD COVERED Final Technical Report	
7. AUTHOR(s) Arthur L. Rousseau Ivo Tammaru	6. PERFORMING ORG. REPORT NUMBER W-08193	
9. PERFORMING ORGANIZATION NAME AND ADDRESS HUGHES AIRCRAFT COMPANY, ELECTRON DYNAMICS DIV 3100 West Lomita Boulevard Torrance CA 90509	8. CONTRACT OR GRANT NUMBER(s) F30602-79-C-0002	
11. CONTROLLING OFFICE NAME AND ADDRESS Rome Air Development Center (OCTP) Griffiss AFB NY 13441	10. PROGRAM ELEMENT, PROJECT, TASK AREA & WORK UNIT NUMBERS 45061245	
14. MONITORING AGENCY NAME & ADDRESS (if different from Controlling Office) Same	12. REPORT DATE February 1982	
	13. NUMBER OF PAGES 54	
	15. SECURITY CLASS. (of this report) UNCLASSIFIED	
	15a. DECLASSIFICATION/DOWNGRADING SCHEDULE N/A	
16. DISTRIBUTION STATEMENT (of this Report) Approved for public release; distribution unlimited.		
17. DISTRIBUTION STATEMENT (of the abstract entered in Block 20, if different from Report) Same		
18. SUPPLEMENTARY NOTES RADC Project Engineer: Joe Polniaszek (OCTP)		
19. KEY WORDS (Continue on reverse side if necessary and identify by block number) Dual Mode High Power TWT		
20. ABSTRACT (Continue on reverse side if necessary and identify by block number) The objective of the MULTIMODE AMPLIFIER program was to perform a feasibility study aimed at the development of a dual power coupled cavity TWT. The characteristics of interest in this device are 100 kW peak power, 10% duty and 500 MHz bandwidth in the primary mode of operation. The secondary mode will have a peak power of 500 kW, bandwidth of 250 MHz and a duty of 10%.		

DD FORM 1 JAN 73 1473 EDITION OF 1 NOV 68 IS OBSOLETE

UNCLASSIFIED

SECURITY CLASSIFICATION OF THIS PAGE (When Data Entered)

**UNCLASSIFIED**

**SECURITY CLASSIFICATION OF THIS PAGE(When Data Entered)**

This report describes the design details of the high power, dual mode S-band TWT and presents performance data from an experimental model, which was constructed to demonstrate some of the design features of the final amplifier. ↗

**UNCLASSIFIED**

**SECURITY CLASSIFICATION OF THIS PAGE(When Data Entered)**

## TABLE OF CONTENTS

<u>Section</u>	<u>Page</u>
1.0 INTRODUCTION	1
2.0 TECHNICAL APPROACH SUMMARY	3
3.0 COLD TESTS AND BASIC CAVITY DESIGN	6
4.0 EXPERIMENTAL RESULTS	15
5.0 DESIGN ANALYSIS AND DUAL MODE PERFORMANCE	34
6.0 CONCLUSIONS AND RECOMMENDATIONS	43

Session For  
1985 CRA&I  
1986 TAB  
1986 Advanced  
1986 Intermediate



## LIST OF ILLUSTRATIONS

<u>Figure</u>	<u>Page</u>
1 Basic cavity design comparison (dimensions in inches).	7
2 Typical $\omega\beta$ curve of 65 kV circuit near condition of merging of main mode and slot mode.	8
3 Measured $\omega\beta$ characteristics of three cold test circuits and the assumed $\omega\beta$ curve of the final design (all with loss buttons).	9
4 Calculated small signal gain vs frequency of a circuit with a nominal design voltage of 75 kV.	11
5 Calculated small signal gain vs frequency of a circuit with a nominal design voltage of 65 kV.	12
6 Assumed interaction impedance of final cavity design.	14
7 598H Experimental S-Band TWT.	16
8 Grid characteristics of 598H, Serial No. 1.	18
9 Power output vs frequency of 598H at a cathode voltage of -50 kV.	19
10 Power output vs frequency of 598H at a cathode voltage of -48 kV.	20
11 Power output vs frequency of 598H at a cathode voltage of -52.5 kV.	21
12 8503H Traveling-Wave Tube.	22
13 8503H, SN-P <sub>3</sub> , power output versus frequency for constant values of input power at a cathode voltage of -39.5 kV, a cathode current of 17A.	24
14 8503H, SN-P <sub>3</sub> , saturated output power versus frequency at a cathode voltage of -39.5 kV for various values of cathode current.	25
15 8503, SN-P <sub>3</sub> , RF input power required for saturation vs frequency at a cathode voltage of -39.5 kV for various values of cathode current.	26

LIST OF ILLUSTRATIONS (CONTINUED)

<u>Figure</u>		<u>Page</u>
16	8503H, SN-P <sub>3</sub> , output power versus frequency at a cathode voltage of -39.5 kV with a constant RF input power of 35 dBm for various values of cathode current.	27
17	8503H, SN-P <sub>3</sub> , saturated output power vs frequency at a cathode voltage of -38 kV for various values of cathode current.	29
18	8503H, SN-P <sub>3</sub> , RF input power required for saturation vs frequency at a cathode voltage of -38 kV for various values of cathode current.	30
19	8503H, SN-P <sub>3</sub> , output power vs frequency at a cathode voltage of -38 kV with a constant RF input power of 38 dBm for various values of cathode current.	31
20	8503H, SN-P <sub>3</sub> , saturated output power vs frequency for various values of cathode voltage with a constant cathode current of 19 amperes.	32
21	8503H, SN-P <sub>3</sub> , RF input power required for saturation vs frequency for various values of cathode voltage at a constant cathode current of 19 amperes.	33
22	Measured and calculated small signal gain vs frequency of the 8503H at three operating conditions.	35
23	Measured and calculated large signal performance of the 8503H.	36
24	Commonality of small signal gain for the 8503H and the dual mode TWT circuits.	38
25	Large signal performance of the dual mode TWT in the low power mode at 54 kV cathode voltage.	39
26	Large signal performance of the dual mode TWT in the high power mode at 62 kV cathode voltage.	40
27	Large signal performance of the dual mode TWT in the high power mode at 61 kV cathode voltage.	41
28	Small signal and saturated gain vs frequency of the dual mode TWT in both modes.	42

## 1.0 INTRODUCTION

There are a number of alternatives to the countering of point jammers in a surveillance scenario. Two obvious approaches are pulse to pulse frequency agility over a wide bandwidth so that the jamming signal is either out of the receiver bandwidth or forced to go wideband and the stepping up of output power combined with the desensitizing of the receiver to effectively "burn through" the point jammer source. The problem that occurs, however, is that neither approach alone results in a complete counter to the point jamming source. A combination of these techniques appears to be the optimum and should result in a point jamming source being countered to such an extent that its threat has been eliminated.

Coupled cavity traveling wave tubes are by their nature relatively wide band devices that are capable of peak power output in the 100 kW to 500 kW range. Deployed in surveillance systems, their wide bandwidth allows both the use of spread spectrum signals and/or pulse-to-pulse frequency agility within the band. If this class of devices could be designed to operate for short time operations (up to 1 second) in a 5:1 power up mode, the preceding approaches to the countering of point jammers could be realized. The net result would be a system which is virtually invulnerable to the point jammer threat.

This program is aimed at the development of a dual power coupled cavity TWT. The characteristics of interest in this device are 100 kW peak power at 10% duty cycle with 500 MHz bandwidth in the primary mode of operation. The secondary or "pulsed up" mode will be of a time duration of 1 second and will be capable of repetition every 30 seconds. The secondary mode will have a peak power output of 500 kW over a bandwidth of 250 MHz at a duty cycle of 10%. All other tube characteristics will remain identical. These objective operating characteristics are listed in Table I.

This report contains the result of the study program. An explanation of the design philosophy is presented. Some of the TWT design features are described. Performance data on experimental TWTs that are related to the dual mode TWT are included. A theoretical analysis of the performance of a tube designed to meet the dual mode requirement is made.

TABLE I  
OBJECTIVE DUAL MODE TWT CHARACTERISTICS

Power Output, Primary Mode	100 kW Peak
Power Output, Primary Mode	10 kW Average
Power Output, Secondary Mode	500 kW Peak
Power Output, Secondary Mode	50 kW Average
Bandwidth, Primary Mode	500 MHz
Bandwidth, Secondary Mode	250 MHz
Time Duration of Secondary Mode	1 Second
Repetition Rate of Secondary Mode	.033 Hz (Once every 30 sec.)
Duty Factor	10%
Center Frequency	3.3 GHz
Pulse Width	Up to 30 Microsec.
Primary Mode to Secondary Mode Switching Time	500 Millisec. Max.

## 2.0 TECHNICAL APPROACH SUMMARY

The chosen technical approach for the high power, dual mode TWT is to use a conventional gridded electron gun together with a coupled-cavity circuit and collector designed to handle the power requirements of the secondary, high power mode. Since this mode represents the greatest thermal load on the tube the design is chosen to optimize the interaction efficiency and beam transmission in this mode. The operating conditions are then adjusted to provide the lower power in the primary mode. The aims of the present program were to study the tradeoffs in the design parameters and tube performance and to determine the modulator and system requirements for the possible modes of operation. It was anticipated that adjustments in grid voltage, cathode voltage and RF input power might be desirable when switching between the primary and secondary modes.

The key features of the tube are the "shadow grid" electron gun, the all copper coupled-cavity interaction circuit and the wrapped-on, integral solenoid to focus the electron beam.

Grid control is essential for transmitter tubes used in modern radars and is particularly necessary to provide the alternate beam power levels required in the dual power tube. The "shadow grid" configuration results in very low current interception on the control grid and allows the control of high power electron beams by low power grid modulators.

The coupled-cavity circuit is inherently a thermally rugged structure. The electron beam could be focused with periodic permanent magnets using iron circuit webs to create the magnetic pole pieces. For the dual mode tube, however, periodic permanent magnet focusing would not be appropriate. The beam transmission is generally not as good with PPM focusing as with solenoid focusing and the iron pole pieces that are a necessary part of the PPM focused coupled cavity circuit have much lower thermal conductivity than copper. Therefore, the very high average power of the dual mode requirement could not

be handled with an S-Band, PPM focused circuit. In addition, since the tube must operate over a range of operating parameters in the different modes, the transmission with PPM focusing would be likely to degrade further and, consequently, degrade the RF performance of the tube as well. For these reasons a solenoid is used to provide the magnetic field to focus the electron beam.

In order to provide good focusing of the electron beam over the two modes of operation magnetic flux from the axial magnetic field will be linked to the cathode to provide semi-confined or "immersed flow" focusing. The field buildup at the cathode must be carefully designed to bring the beam to the correct condition at the entrance of the slow wave circuit. The proper amount of flux linking the cathode surface also has a "stiffening" effect on the focusing under RF large signal conditions. This minimizes RF defocusing at the output of the tube.

To reduce the size and power requirement of the solenoid, the solenoid windings are wound directly onto the body of the tube. This results in a smaller solenoid bore, since it does not have to be large enough to pass over the outer diameter of the electron gun. It also results in excellent alignment between the solenoid and the tube circuit. The individual solenoid turns can be adjusted independently during test to optimize the beam entrance condition.

A basic consideration at the start of the study was that the tube should be designed to operate with as low a beam perveance as possible, since lower perveance generally results in better beam focusing and reduced focusing field requirements, higher circuit interaction efficiency, and simpler electron gun structures. There is also less variation in the dc beam velocity between two current modes because of lower space charge depression in the beam. This would minimize any required cathode voltage adjustments between the two modes. A drawback to the lower perveance design would be that it would result in a higher cathode voltage.

For this application, however, the operating perveance cannot be arbitrarily reduced. A fundamental characteristic of the conventional coupled cavity circuit is that the available bandwidth of the interaction mode is reduced as the voltage of the circuit is increased. The circuit bandwidth is a rather complicated function of the entire geometry of the cavity and, therefore, is generally determined experimentally rather than by calculation. Consequently, one of the first tasks of the program was to fabricate experimental cavity structures and measure their characteristics to determine the maximum cathode voltage for the dual mode tube that would be compatible with the bandwidth requirements.

After the appropriate operating voltage was determined, computer calculations were made of the expected performance of the final design.

RF measurements were made on experimental TWTs having some design features similar to the dual mode tube to demonstrate these features and to verify the accuracy of the computer calculations.

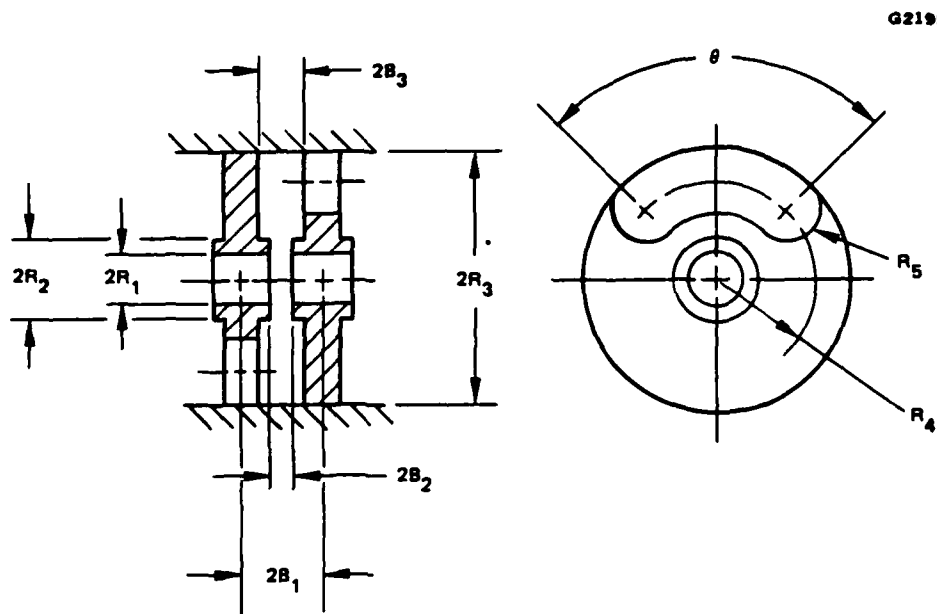
Discussions of some of these design features, results of the experimental measurements, theoretical analysis of the final design, and conclusions and recommendations are included in the following sections.

### 3.0 COLD TESTS AND BASIC CAVITY DESIGN

Frequency versus phase ( $\omega\theta$ ) measurements were made on two basic cold test circuit structures. These circuits were designed for nominal cathode voltages of 75 kV (Design I) and 65 kV (Design II). The dimensions of the circuits are listed in Figure 1. The frequency measurements determine the passband of the main fundamental mode of the cavity structure as well as the passband of the next higher order mode, which is associated with the resonant frequency of the kidney shaped coupling slot between adjacent cavities. As mentioned previously, it was felt that it would be desirable to design the dual mode tube to operate at a low beam perveance (i.e. high cathode voltage); however, the limitation on how low a perveance can be used depends upon the required bandwidth. The bandwidth of the coupled cavity circuit is increased by increasing the width of the coupling slot by enlarging the angle  $\theta$  of Figure 1. But as the bandwidth of the fundamental mode is increased in this manner, the bandwidth of the "slot" mode is also increased and the slot mode frequency band shifts closer to the fundamental mode, until eventually the two modes merge. This merged mode condition represents the limit of the maximum bandwidth for the fundamental mode. The circuit geometry required for higher voltage operation, such as a larger period, generally results in the bandwidth limit being narrower. The purpose of the cold test circuit measurements was to determine how high an operating voltage could be possible while still providing the required bandwidth.

A series of measurements were made on both basic circuits with successively larger coupling slots. A typical curve is shown in Figure 2. This curve is for the nominal 65 kV circuit with the coupling slot opened to the point where the bandwidth is close to the merged mode condition. The circuit in this case had no loss buttons, which actually must be incorporated to ensure stability.

Data taken on three circuits with buttons are displayed in Figure 3 (the curves with cavity period of 1.180 or 1.260 inches). Because the buttons are lossy and are designed to resonate around the upper cutoff frequency of the lowest passband, the  $\omega\theta$  curve is ill defined in that region.



	Design I (75 kV)	Design II (65 kV)
Ferrule ID (2R <sub>1</sub> )	0.564	0.520
Cavity Dia. (2R <sub>3</sub> )	1.440	1.420
Circuit Period (2B <sub>1</sub> )	1.260	1.180
Cavity Height (2B <sub>3</sub> )	1.040	0.960
Web Thickness 2(B <sub>1</sub> - B <sub>3</sub> )	0.220	0.220

Figure 1 Basic cavity design comparison (dimensions in inches).

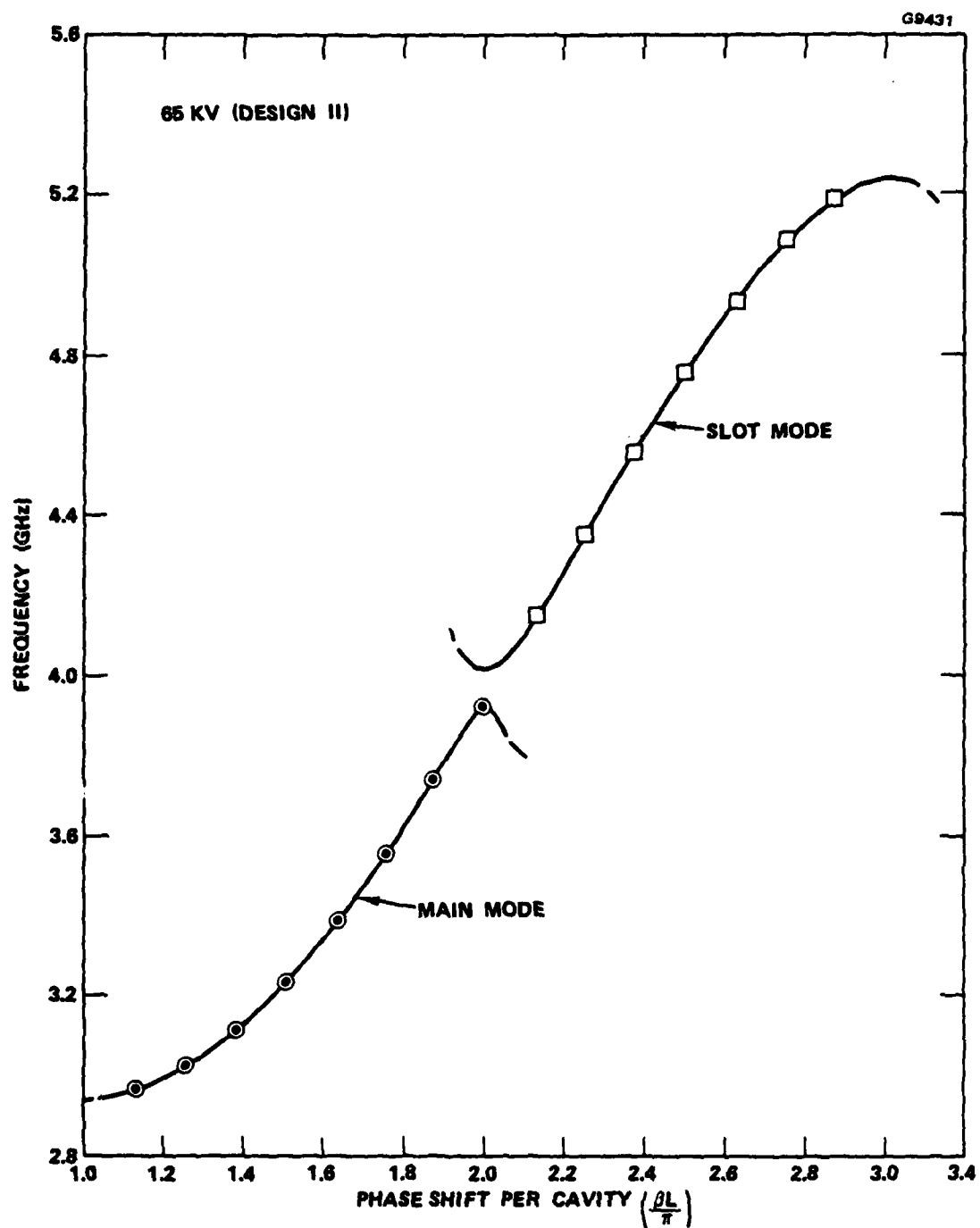


Figure 2 Typical  $\omega\beta$  curve of 65 kV circuit near condition of merging of main mode and slot mode.

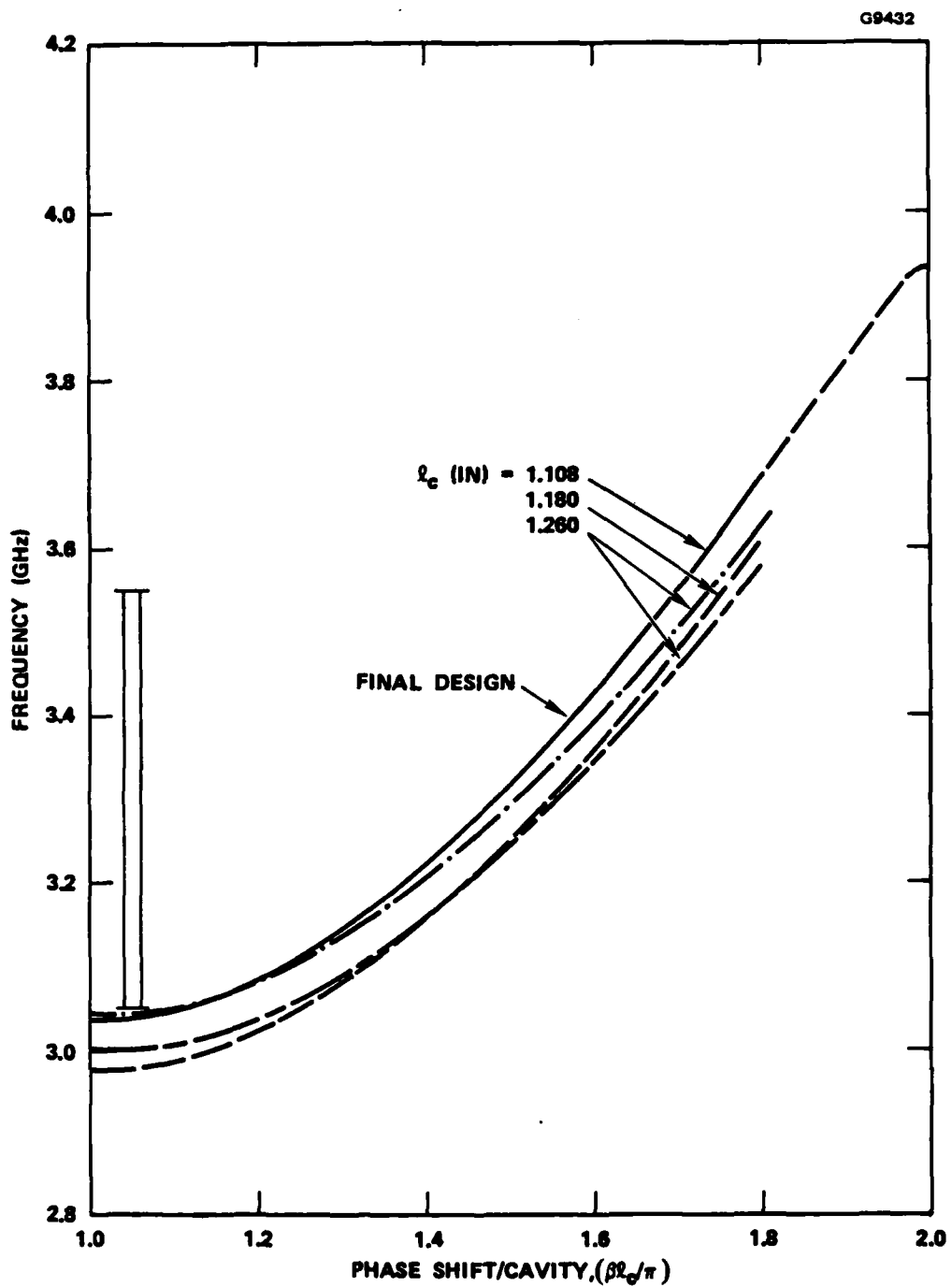


Figure 3 Measured  $w\beta$  characteristics of three cold test circuits and the assumed  $w\beta$  curve of the final design (all with loss buttons).

Preliminary small signal gain calculations were made using the two lowest curves of Figure 3. Uniform circuits with three sections were evaluated. The results are shown in Figure 4 for the nominal 75 kV design (period 1.260") and in Figure 5 for the 65 kV design (period 1.180"). The beam power in the high mode was taken to be 2 MW, assuming 25 percent efficiency, and 600 kW in the low mode, corresponding to an efficiency of 17 percent. The circuit with a period of 1.26, Figure 4, is too limited on bandwidth; it was actually also beyond the merged mode condition, which accounts for the rapidly dropping gain toward the high frequency end. Because of the high perveance in the high power mode, there is significant space charge depression in the beam. The electron velocity is consequently reduced. To establish the same axial electron velocity as in the low power mode, and thus a similar gain versus frequency variation, the cathode voltage must be increased in the high power mode. The figure also illustrates how the frequency response shifts up when only the beam current is increased. The 65 kV circuit, Figure 5, is appreciably better, but wider small signal gain bandwidth would be preferred.

At this point, the analytical investigations were suspended, awaiting test results on two related TWTs. The performance of these tubes is described in the next section. Concerning the basic cavity design, the following two conclusions from the experimental data were relevant: First, the shadow gridded electron gun, with nominal beam perveance of 2.0, could be reliably operated at a perveance approaching 2.6 with good beam focusing (97 percent DC transmission and 91 percent with RF, without any special effort to optimize the focusing at the high perveance operation). The voltage in the high mode could consequently be reduced to about 62 kV while yet providing sufficient beam power. This allowed a reduction in the cavity period making it possible to obtain a larger cold bandwidth and thus increase the RF performance bandwidth. Secondly, good gain and output power with sufficient margin was demonstrated down to the low frequency cutoff of the basic cavity circuit. A similar design was planned for the dual mode tube.

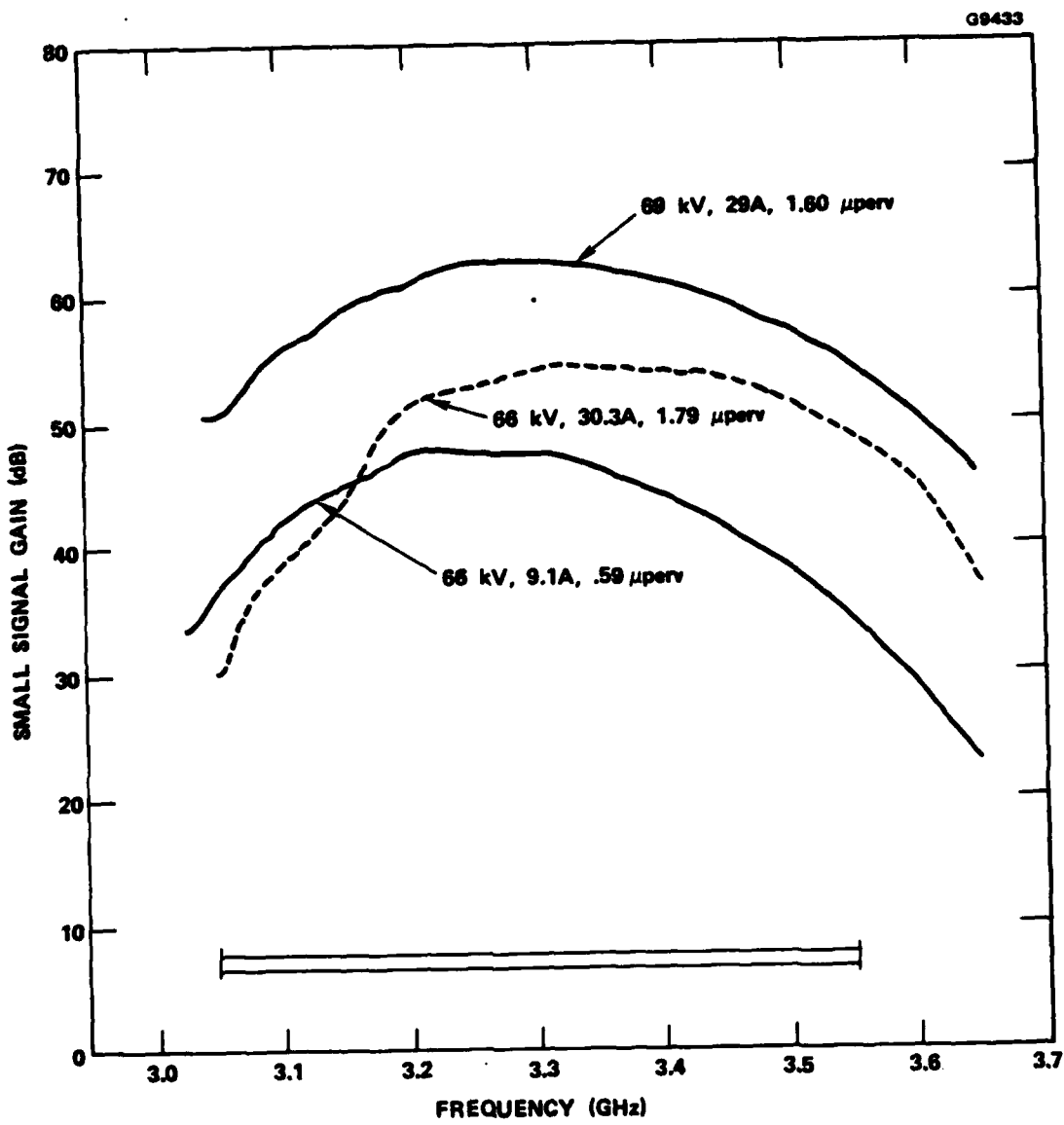


Figure 4 Calculated small signal gain vs frequency of a circuit with a nominal design voltage of 75 kV.

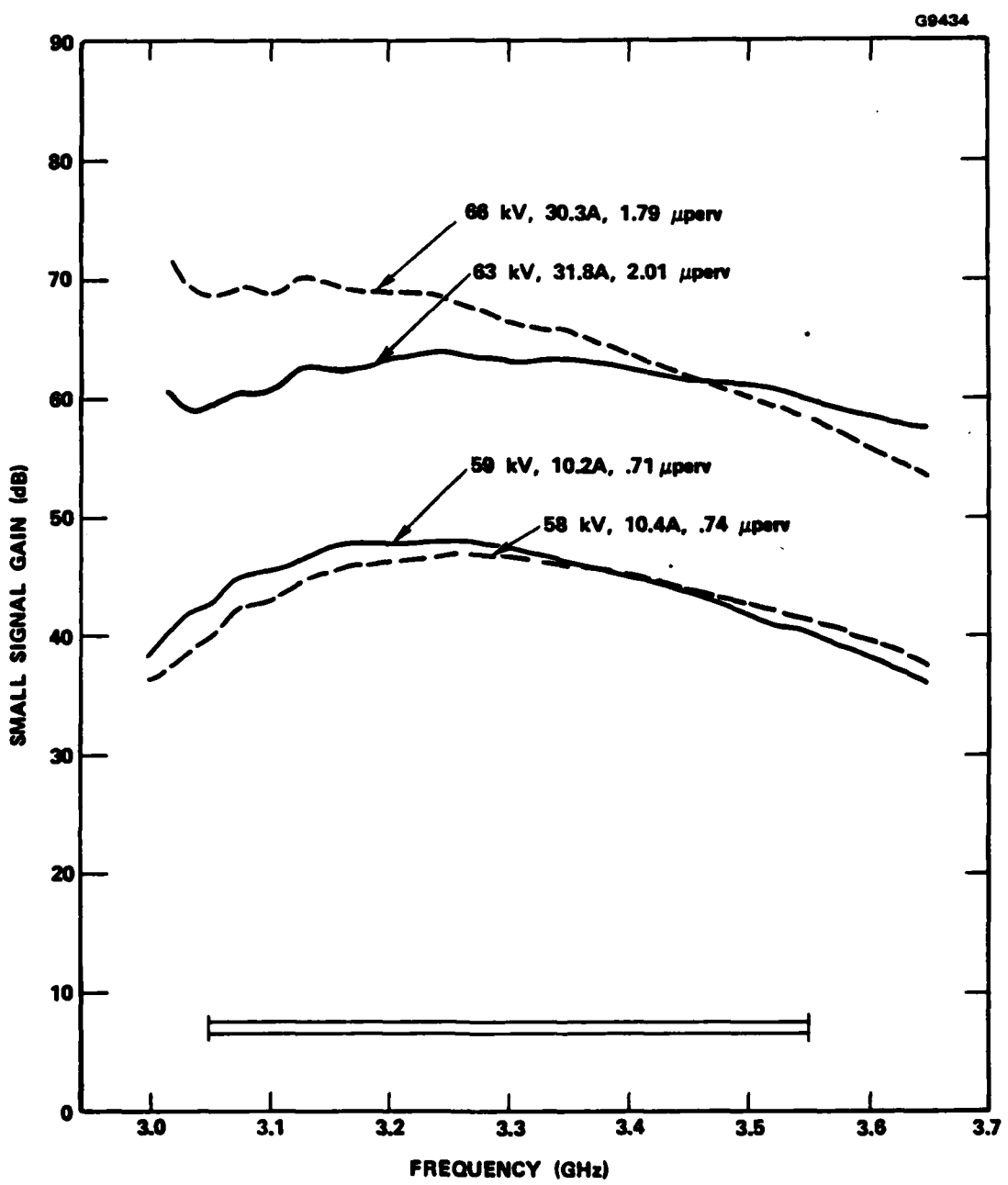


Figure 5 Calculated small signal gain vs frequency of a circuit with a nominal design voltage of 65 kV.

Figure 3 includes the  $\omega\beta$  characteristic constructed for the final cavity design, assuming a period of 1.108" and beam hole of .520". Although the design was not verified by cold tests, there should be no problem in achieving it, judging from the trends of the measured curves on circuits with longer cavity periods. The Pierce interaction impedance, with beam filling factor of .75 and confined flow, is plotted in Figure 6 for the final design. It is consistent with the measured impedance of the cold test circuits.

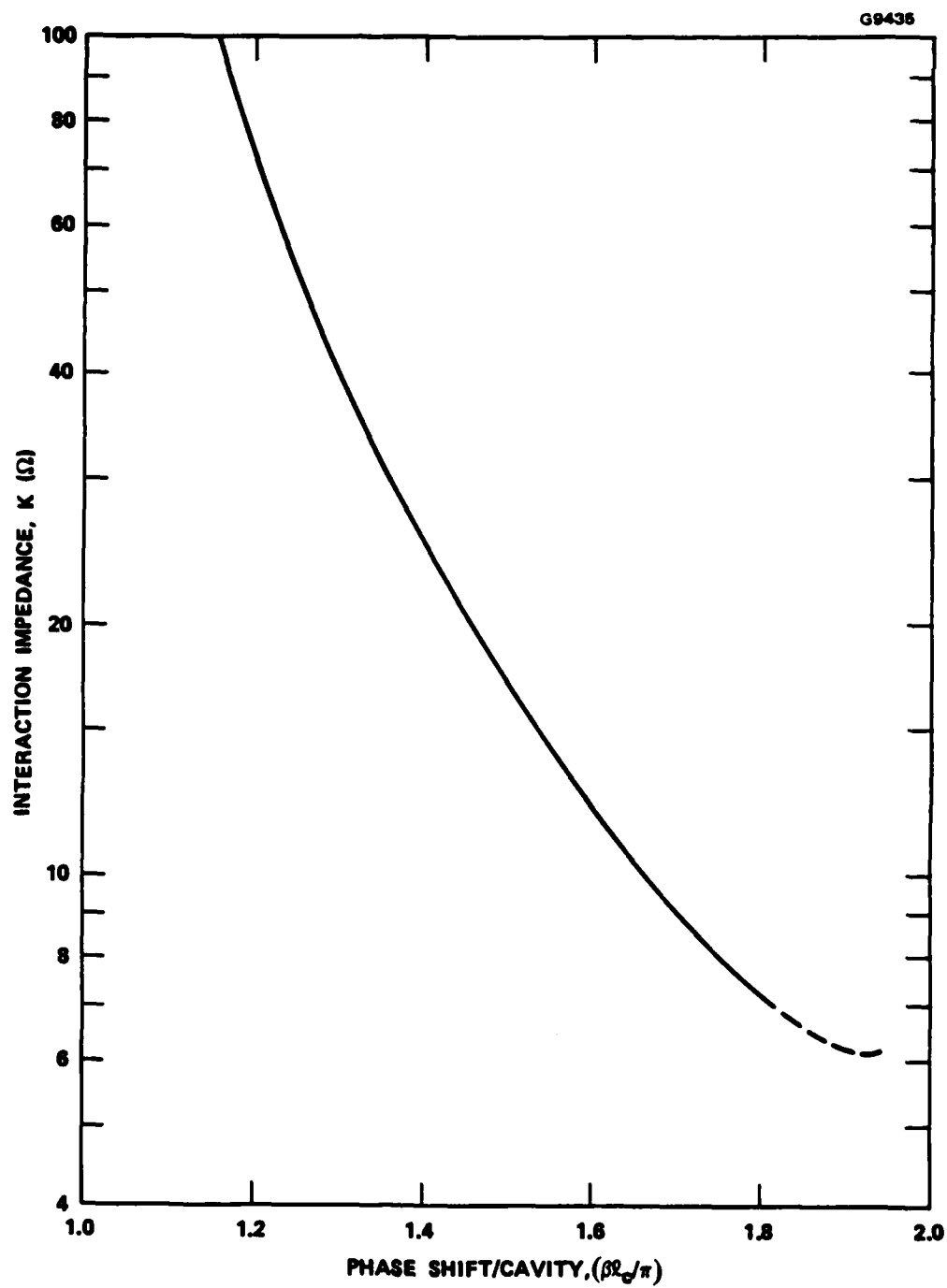


Figure 6 Assumed interaction impedance of final cavity design.

#### 4.0 EXPERIMENTAL RESULTS

Measurements were made on two solenoid focused, S-band, coupled-cavity TWTs to obtain empirical data in order to realistically calibrate the computer calculations. These measurements also verify that the operating parameters of the tube could be varied over sufficient ranges to provide dual mode performance while still maintaining tube stability. The tubes that were evaluated were the Hughes 598H and 8503H.

##### 598H

The 598H is a developmental, S-band, coupled-cavity TWT designed for a power output of 250 kW peak. It uses a shadow-gridded electron gun. The beam is focused by an integral wrapped solenoid. The nominal cathode voltage is -50 kV at a cathode current of 22 amperes. Figure 7 is a photograph of the 598H.

Unfortunately, the one experimental model that was constructed had a number of problems that prevented it from operating very well. The test data could not be used to draw any conclusions about the dual mode performance of such a device. The major problem was that the gun entrance conditions to the magnetic field were incorrect so that the beam transmission was poor. Another problem was that the tube had large gain variations, which resulted in oscillations under some operating conditions. Many adjustments of the individual solenoid turns were tried to optimize the tube performance. A bucking coil around the electron gun was also used. Some operating data were obtained. However, the solenoid settings that had to be used to obtain beam transmission better than 90 percent and to eliminate the oscillations resulted in very low gain. Saturated output power could not be obtained over the whole bandwidth with the 20 watt driver that was available.

E3426



Figure 7 598H Experimental S-Band TWT.

The grid characteristics are shown in Figure 8. Power output versus frequency for constant RF input power at different values of cathode voltage are presented in Figures 9, 10 and 11. These data were taken at low duty cycle. A wider range of parameters was not investigated because the focusing performance was poor and a driver was not available to saturate the tube.

Modifications could be made in successive models of the 598H to improve the performance. Such changes have already been made in later models of the 8503H (which is a related, lower power TWT, that will be described in the next section). These changes would involve adjusting the entrance conditions of the electron gun to the magnetic field and improving the RF match of the circuit to correct the gain variations. Possibly, the number of circuit cavities would be increased to raise the gain.

#### 8503H

The 8503H is an S-band TWT that is closely related to the dual mode tube and the 598H, but at a lower power level. It is designed for a peak power output of 125 kW over the frequency band of 3.1 to 3.5 GHz. It operates at a nominal cathode voltage of -40 kV at a cathode current of 17 amperes. The electron gun of the 8503H is identical to the 598H electron gun. The circuit period is scaled to operate at the lower voltage and power level. Figure 12 is a photograph of the 8503H.

The first model of the 8503H that was built had performance problems similar to those of the 598H. However, modifications were made in the successive models of the 8503H to improve the beam transmission and stability. It was possible to operate 8503H, serial number P3, over a wide range of beam voltages and currents. The gain was reasonable. There were no oscillation problems. Data from this tube serve as the basis for the theoretical calculations of the performance of the final dual mode tube design.

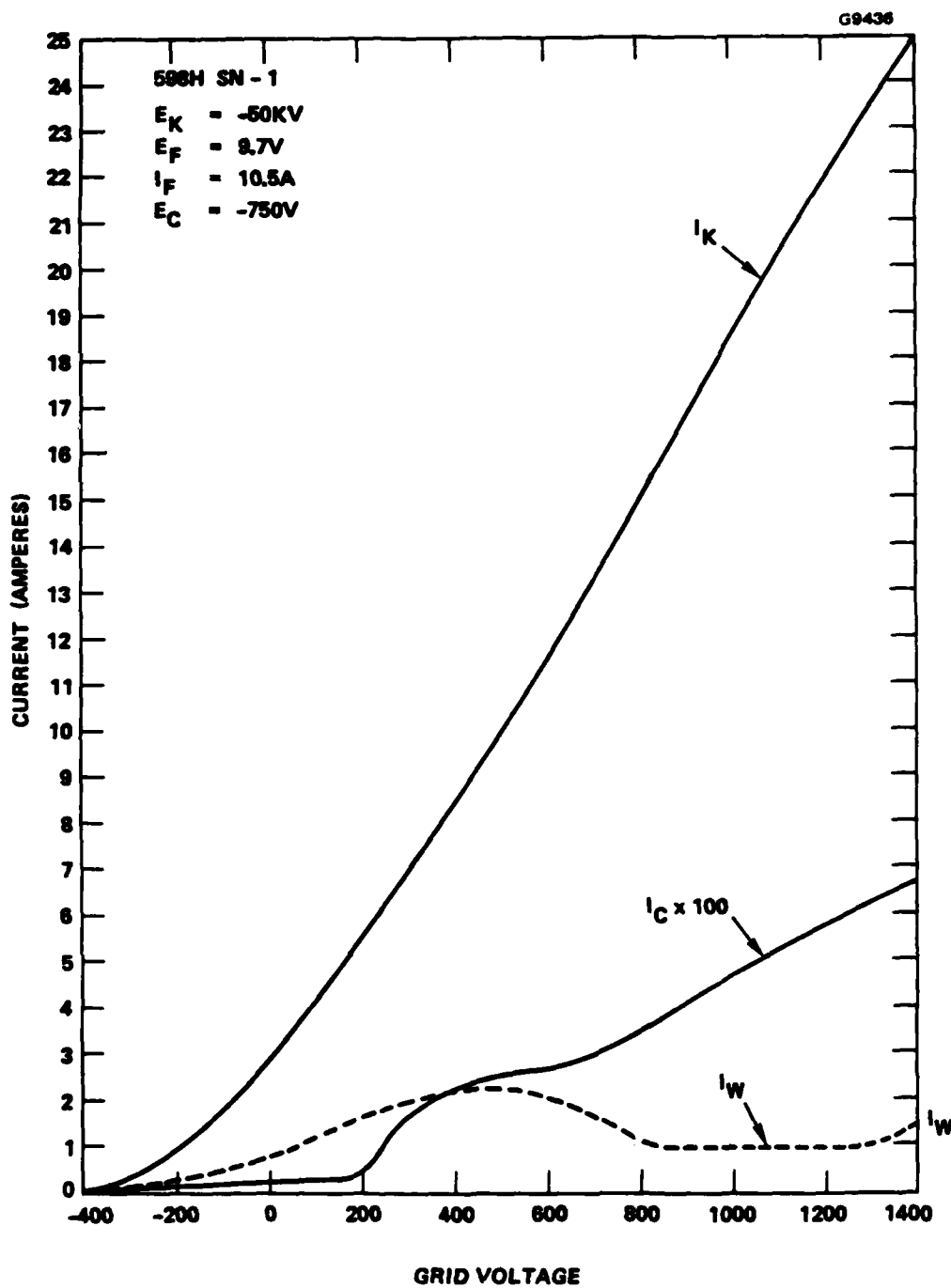


Figure 8 Grid characteristics of 598H, Serial No. 1.

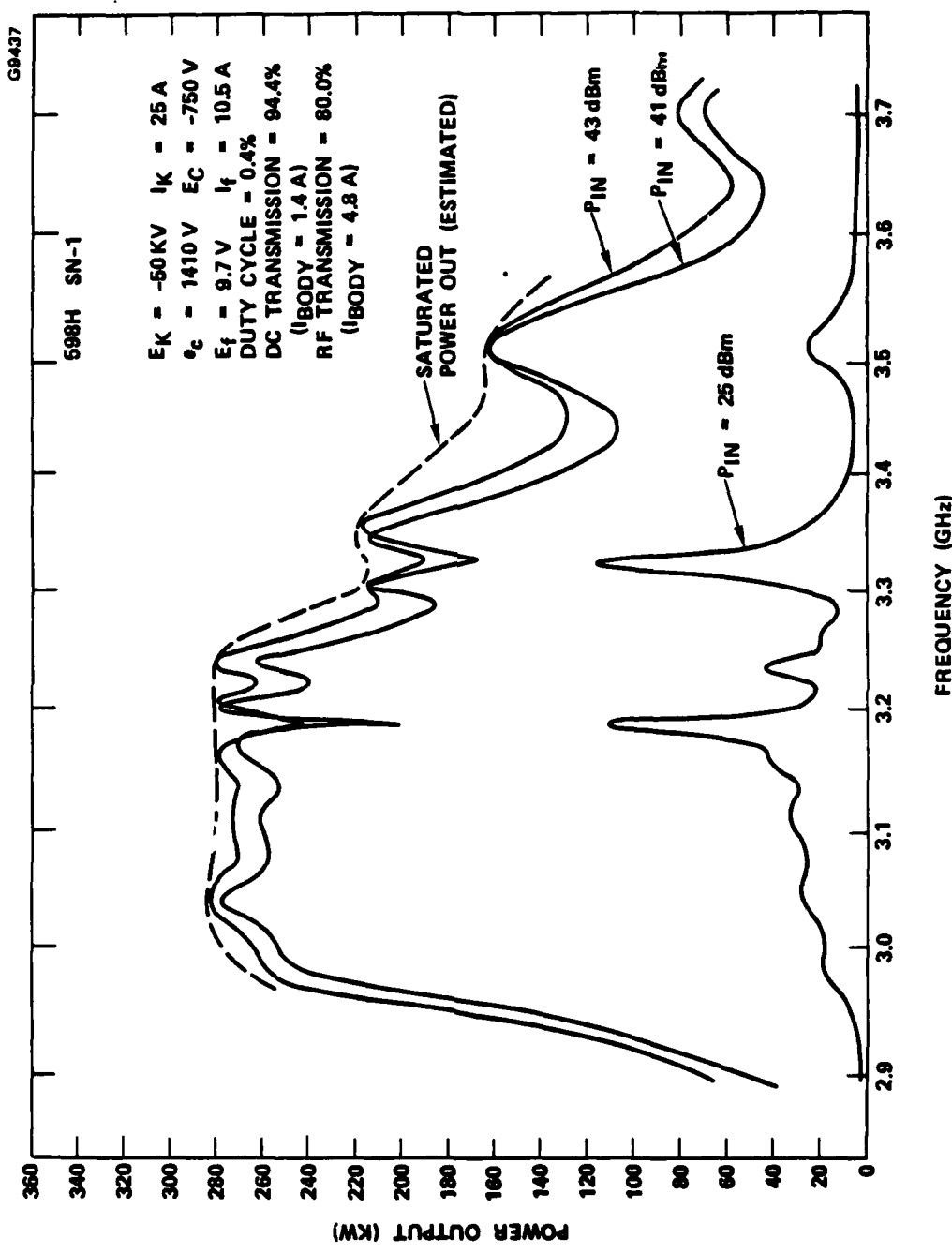


Figure 9 Power output vs frequency of 598H at a cathode voltage of -50 kV.

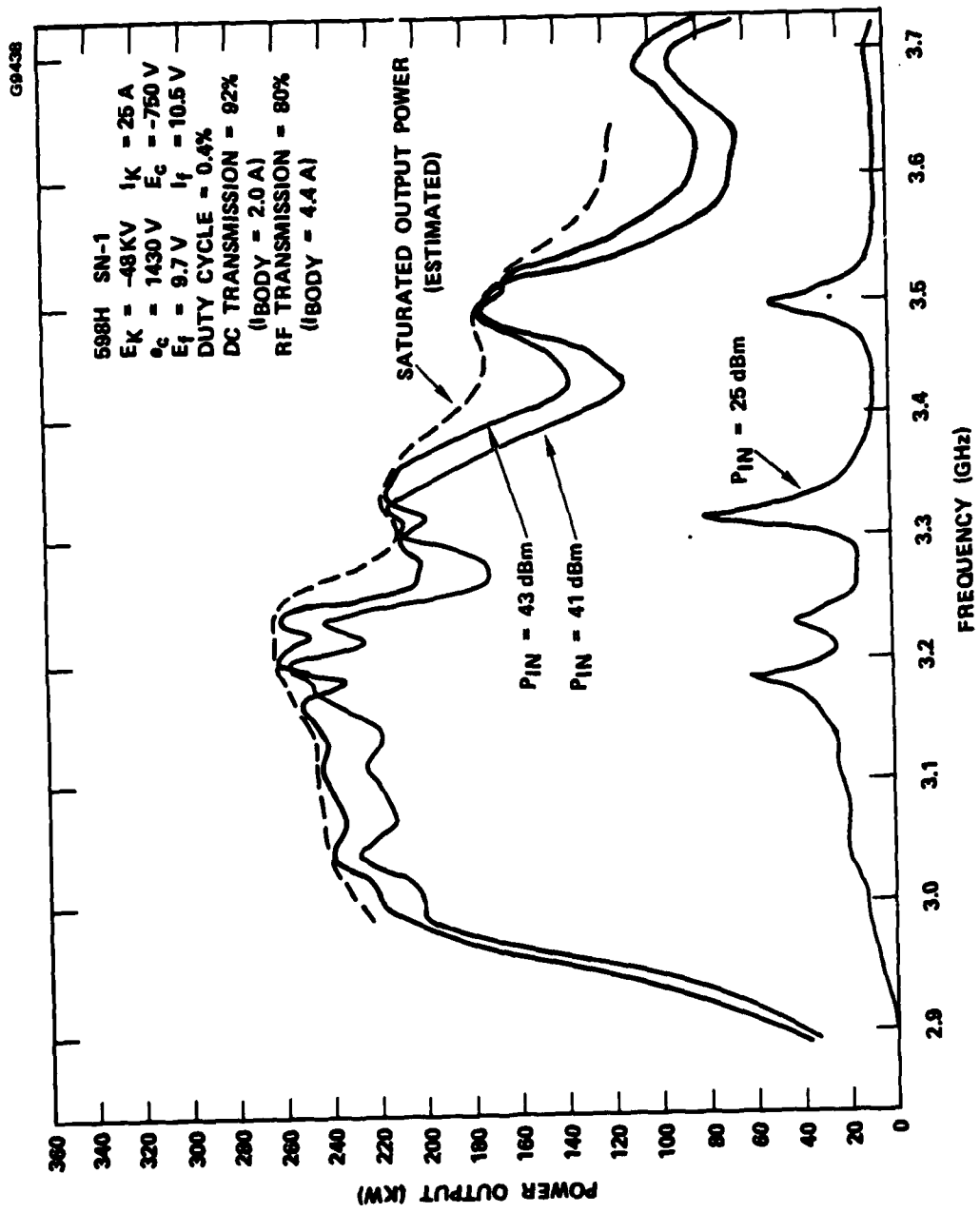


Figure 10 Power output vs frequency of 598H at cathode voltage of -48 kV.

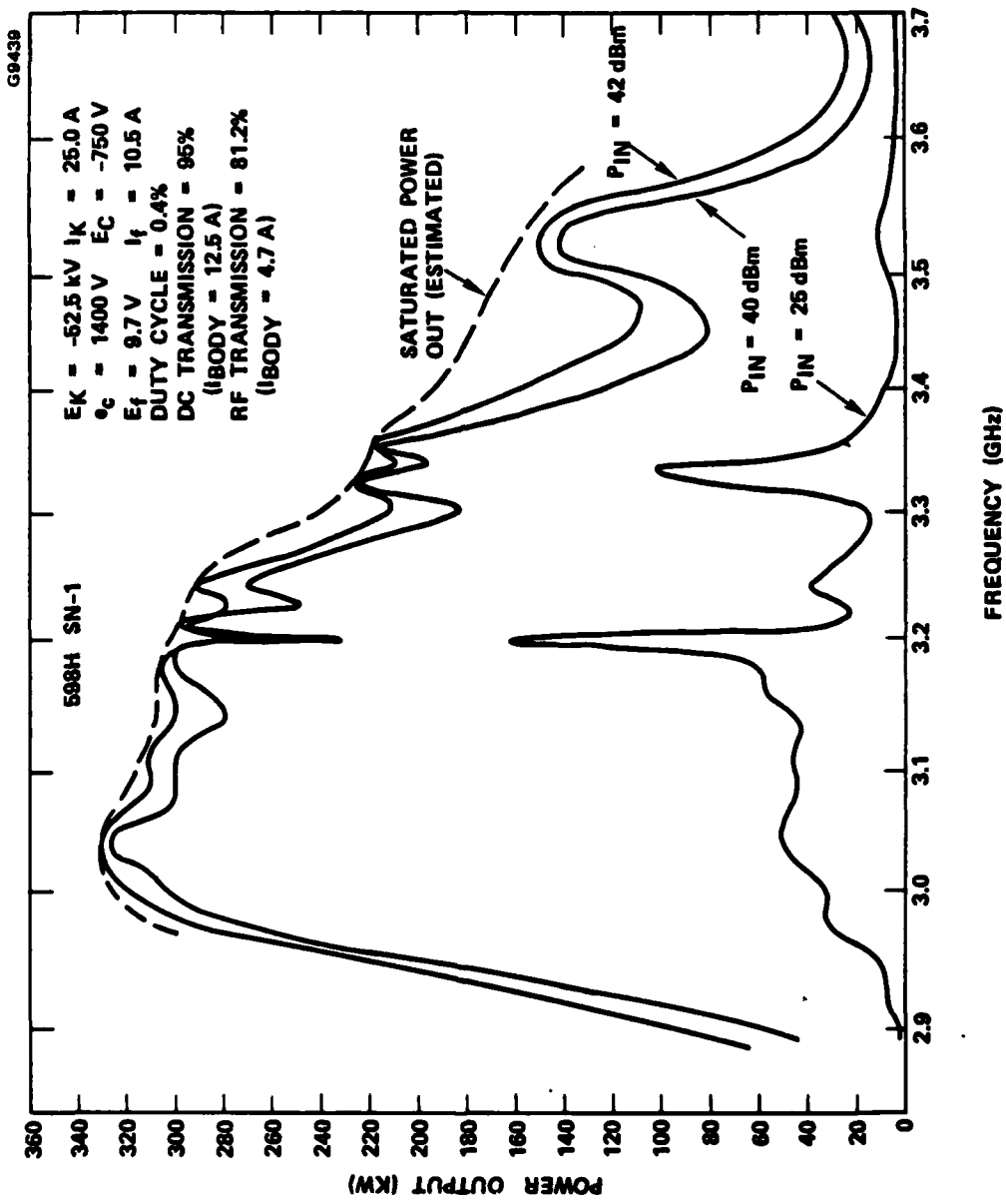


Figure 11 Power output vs frequency of 598H at a cathode voltage of -52.5 kV.

E3427



Figure 12 8503H Traveling-Wave Tube.

The 8503H, serial number P3, was tested over a range of operating parameters from a cathode voltage of -35 kV at a beam current of 8 amperes to a cathode voltage of -49 kV at 20 amperes. Some of this performance is summarized in the following curves.

Figure 13 shows swept power output versus frequency for constant values of RF input at a cathode voltage of -39.5 kV and a beam current of 17 ampres. These are the nameplate operating parameters for this tube. From these data the saturated power output and RF input power required for saturation can be obtained.

At -39.5 kV cathode voltage the beam current was varied in steps from 5 amperes to 20 amperes by varying the grid pulse voltage. No other adjustments were made. Families of power output curves similar to those at 17 amperes were generated. From these curves the saturated power output as a function of beam current was obtained. These curves are shown in Figure 14. Where the available RF input was not large enough to reach saturation, the extrapolated value of saturated power is indicated by the dashed portion of the curves.

Figure 15 shows the RF input levels required for saturation. At this cathode voltage (-39.4 kV) there is a relatively small change in drive required for the entire range of beam currents from 5 to 20 ampere. This is illustrated in Figure 16 which shows power output versus frequency with various values of beam current at a constant RF input level of 35 dBm. Note that a 20 amperes greater than 160 kW of peak output power is obtained over a relatively broad bandwidth of 3.05 to almost 3.7 GHz. At 5 amperes, the peak power is about 30 kW over a narrower frequency band. Only the grid voltage was changed between the curves. There was no attempt made to vary the focusing solenoid current to optimize the power output at the different current levels.

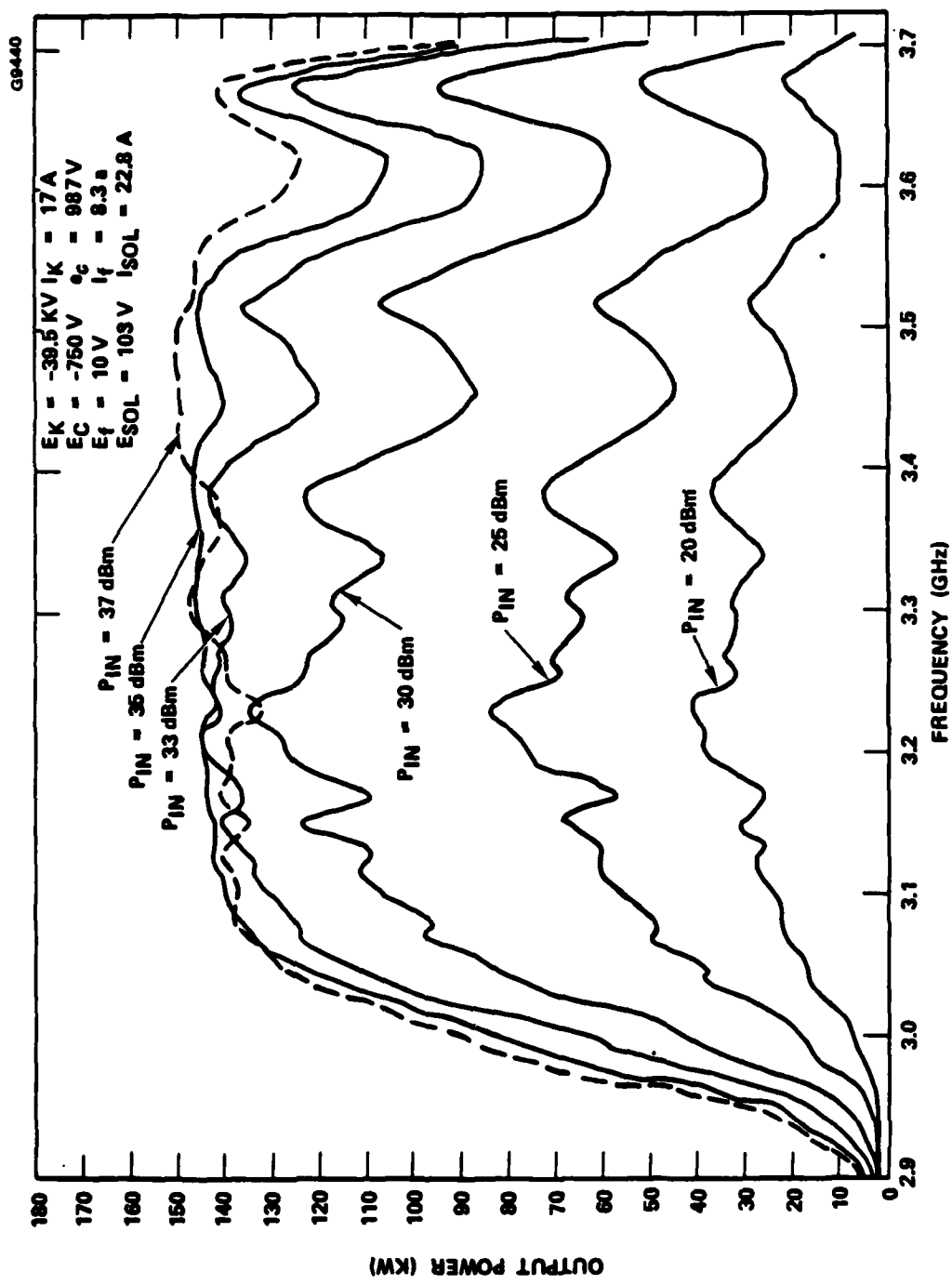


Figure 13 8503H, SN-P3, power output versus frequency for constant values of input power at a cathode voltage of -39.5 KV, a cathode current of 17A.

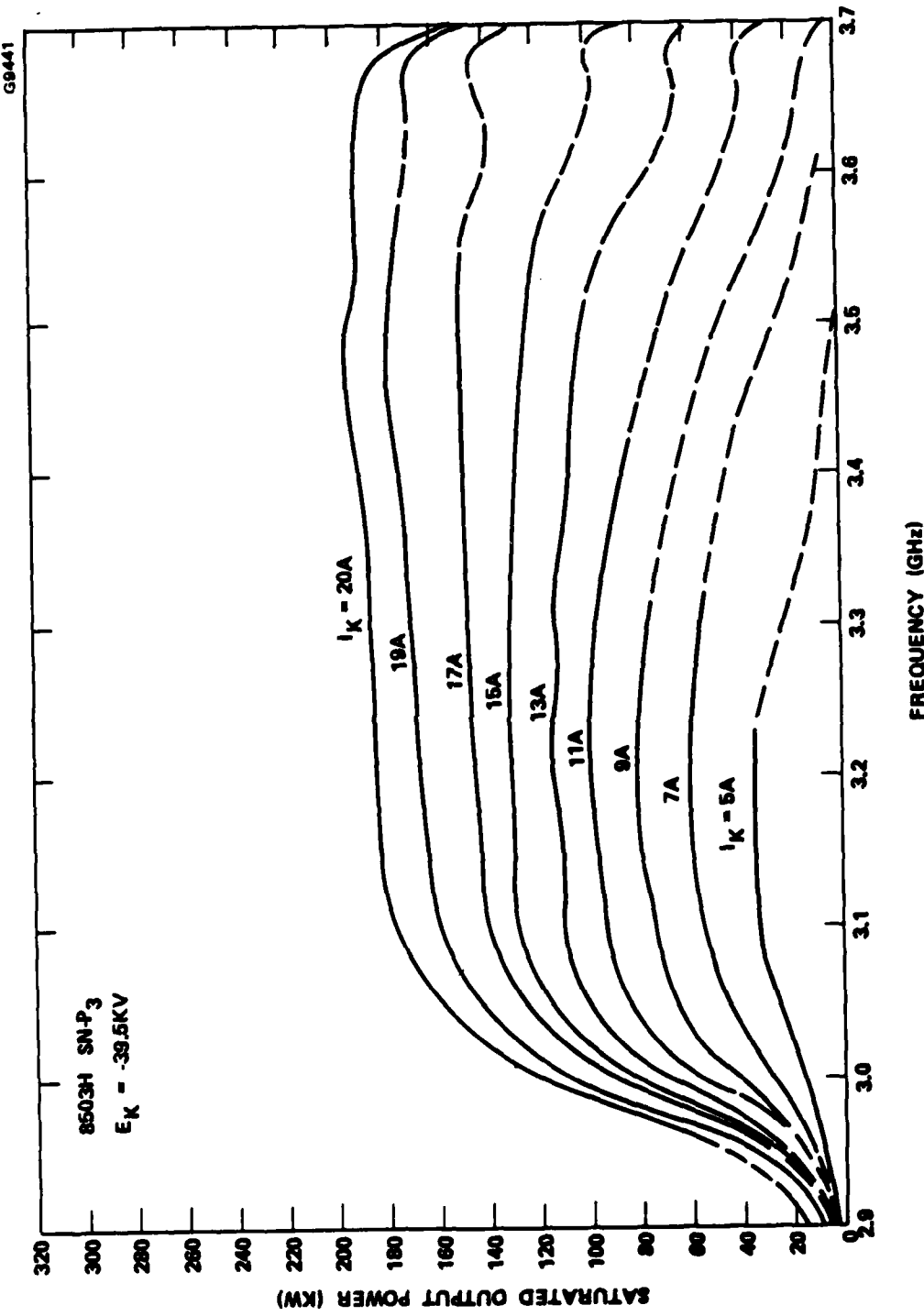


Figure 14 8503H, SN-P3 saturated output power versus frequency at a cathode voltage of -39.5 kV for various values of cathode current.

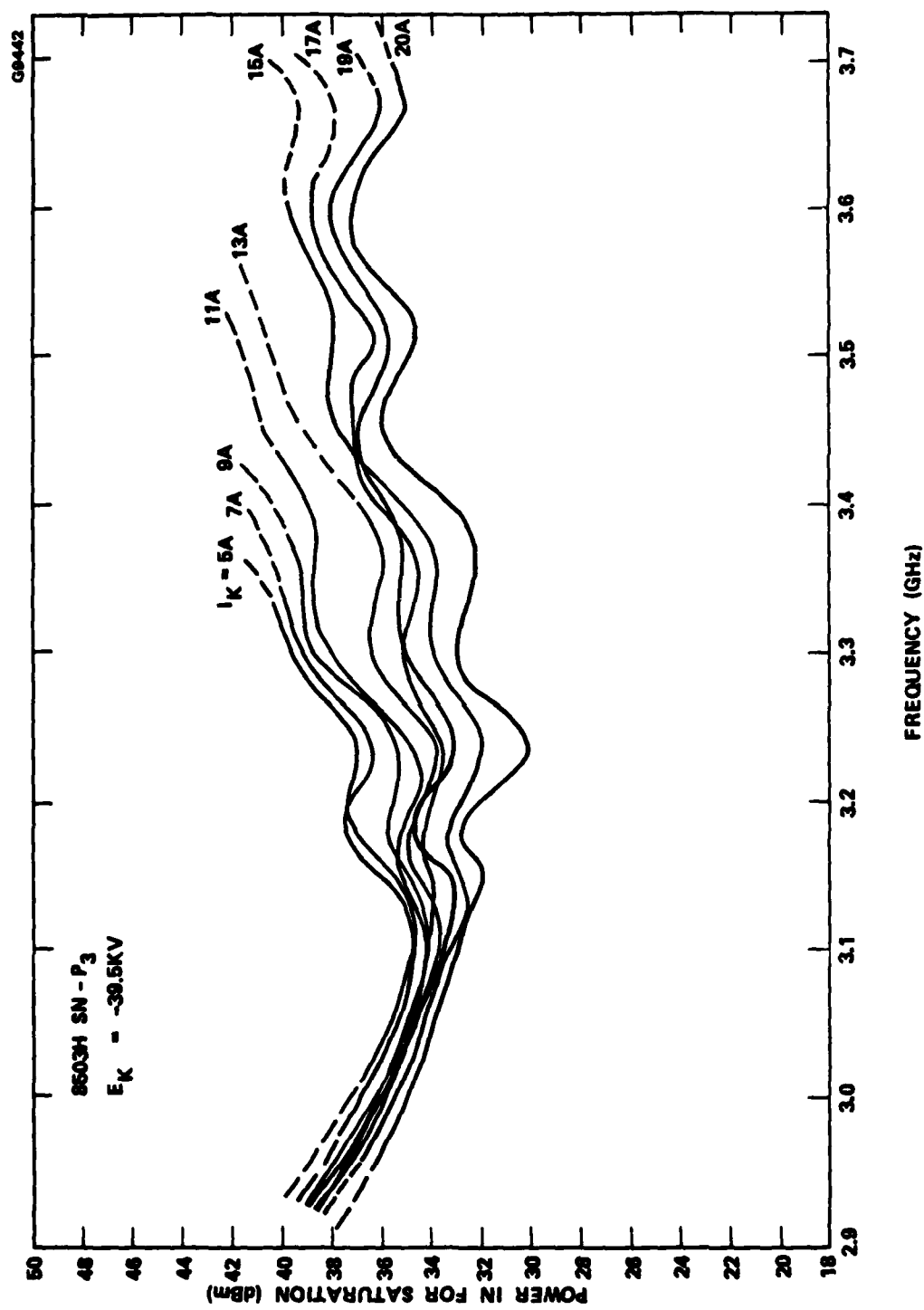


Figure 15 8503H, SN-P<sub>3</sub>, RF input power required for saturation vs frequency at a cathode voltage of  $-39.5\text{ kV}$  for various values of cathode current.

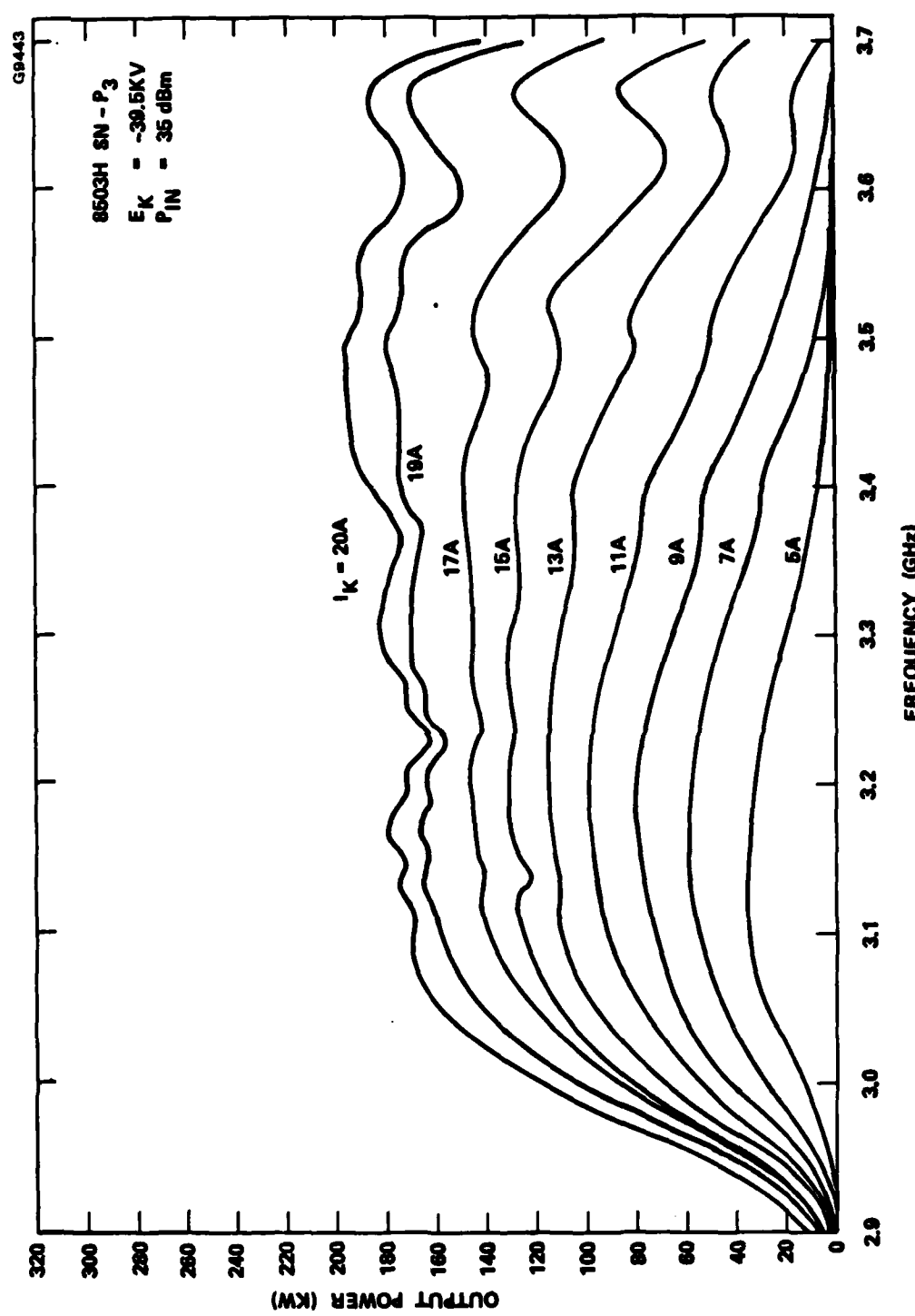


Figure 16 8503H, SN-P<sub>3</sub>, output Power versus frequency at a cathode voltage of -39.5 kV with a constant RF input power of 35 dBm for various values of cathode current.

Similar measurements were at a lower cathode voltage of -38 kV. Saturated power output for a range of beam currents from 5 amperes to 19 amperes is presented in Figure 17. As before, the dashed portions of the curves indicate that the RF input drive that was available when the tests were performed was not sufficient to obtain saturates power out, so those portions of the curves are extrapolated.

RF input power required for saturation is shown in Figure 18.

RF output versus frequency for various values of beam current with a constant RF input of 38 dBm is shown in Figure 19 at the cathode voltage of 38 kV. The bandwidth is not quite as broad as at -39.5 kV, but still respectable performance was obtained with an approximately 5 to 1 change in power level by only making the simple adjustment of varying the grid voltage.

As the cathode voltage is increased greater power output was obtained. However, the gain variations become larger (or with a constant RF input power the bandwidth is narrower). From the swept power output curves, the saturated output power was obtained as before for various values of cathode voltages from -38 kV to -48 kV with the grid drive adjusted to provide a constant cathode current of 19 amperes. This is presented in Figure 20.

In Figure 21, the RF input levels required to obtained the saturated output power for that range of cathode voltages. Over 30 dB of RF input adjustment is required to get saturated output power over this range of cathode voltages.

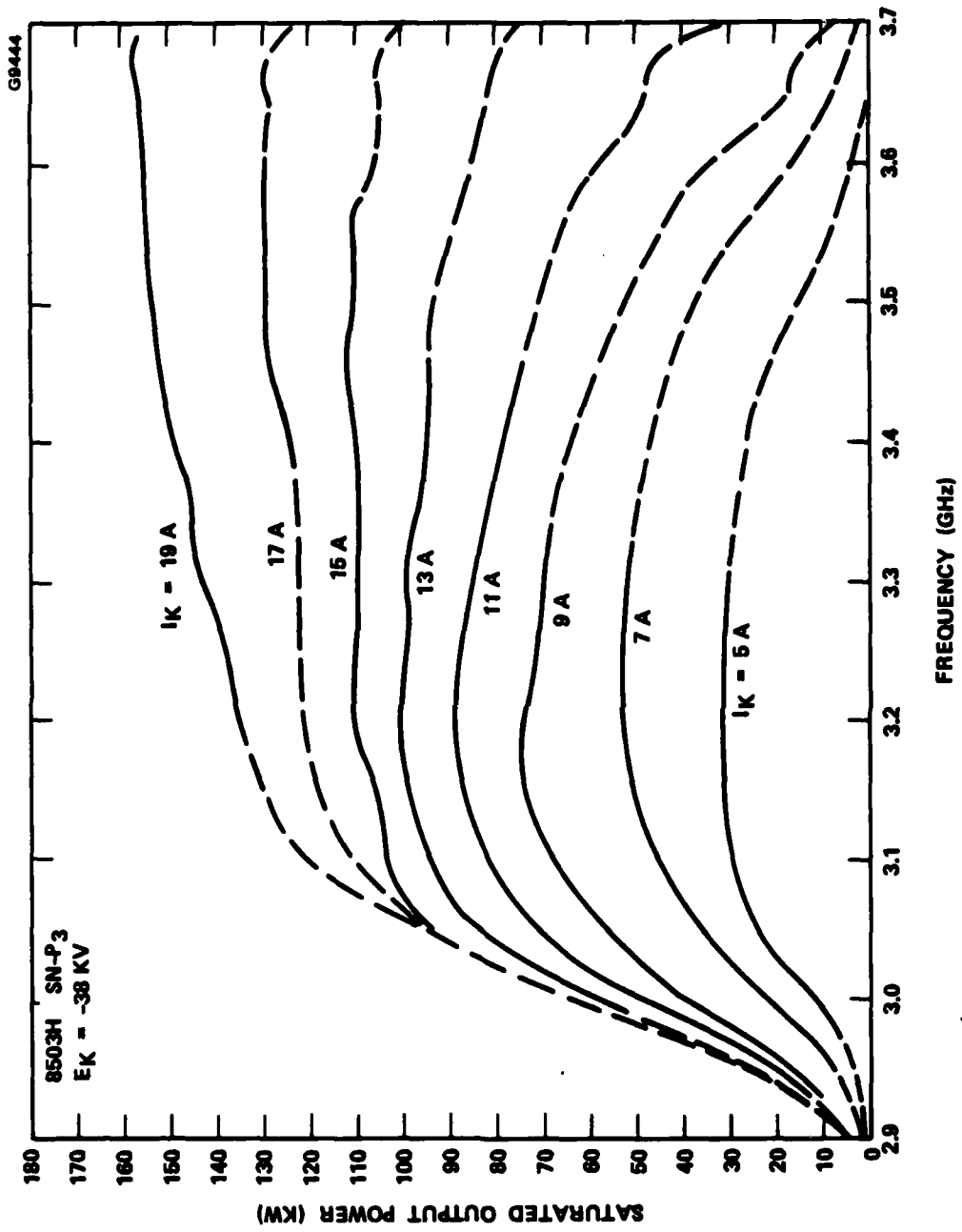


Figure 17 8503H, SN-P3, saturated output power vs frequency at a cathode voltage of -38 KV for various values of cathode current.

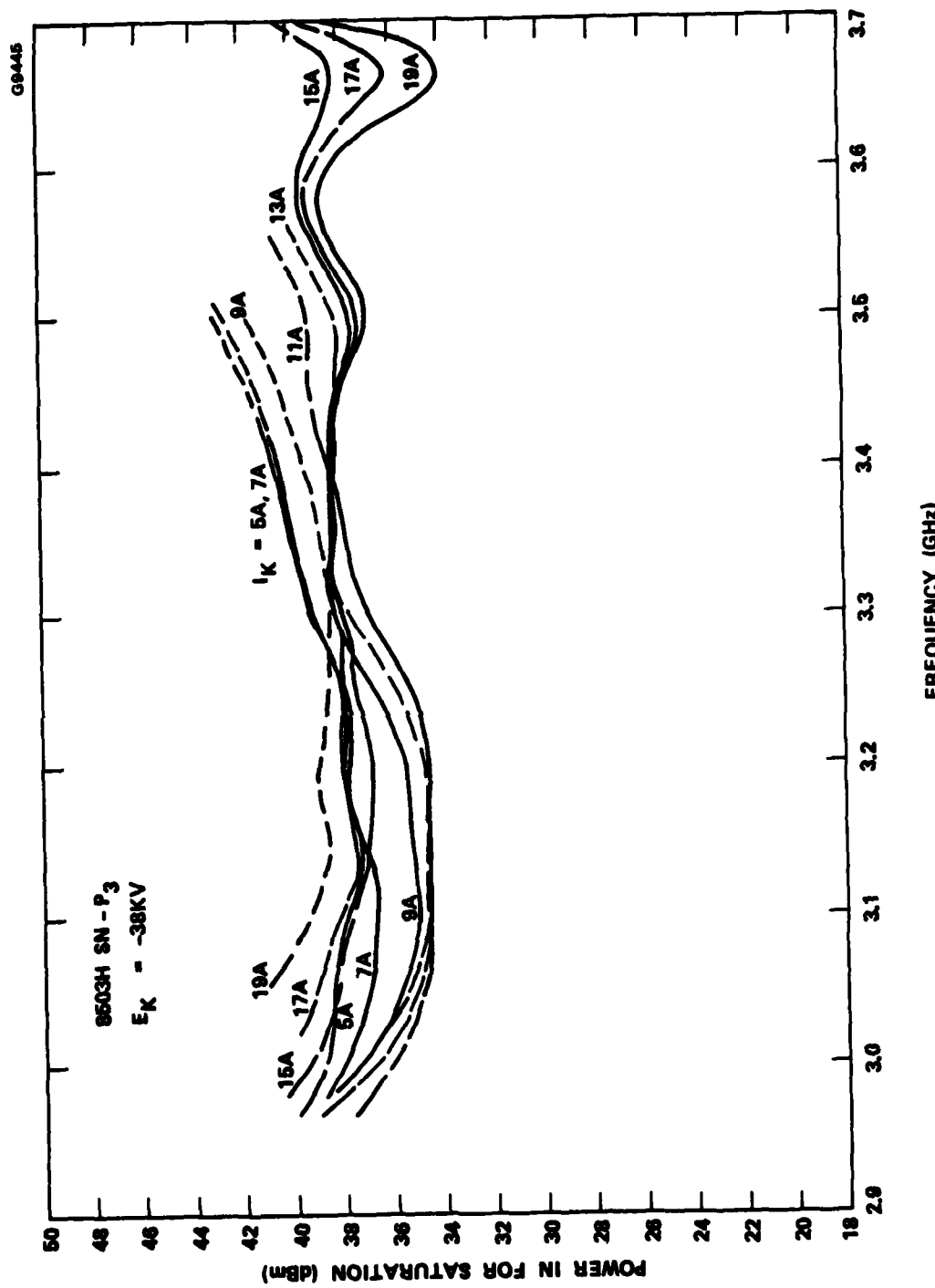


Figure 18 8503H, SN-P<sub>3</sub>, RF input power required for saturation vs frequency at a cathode voltage of -38 kV for various values of cathode current.

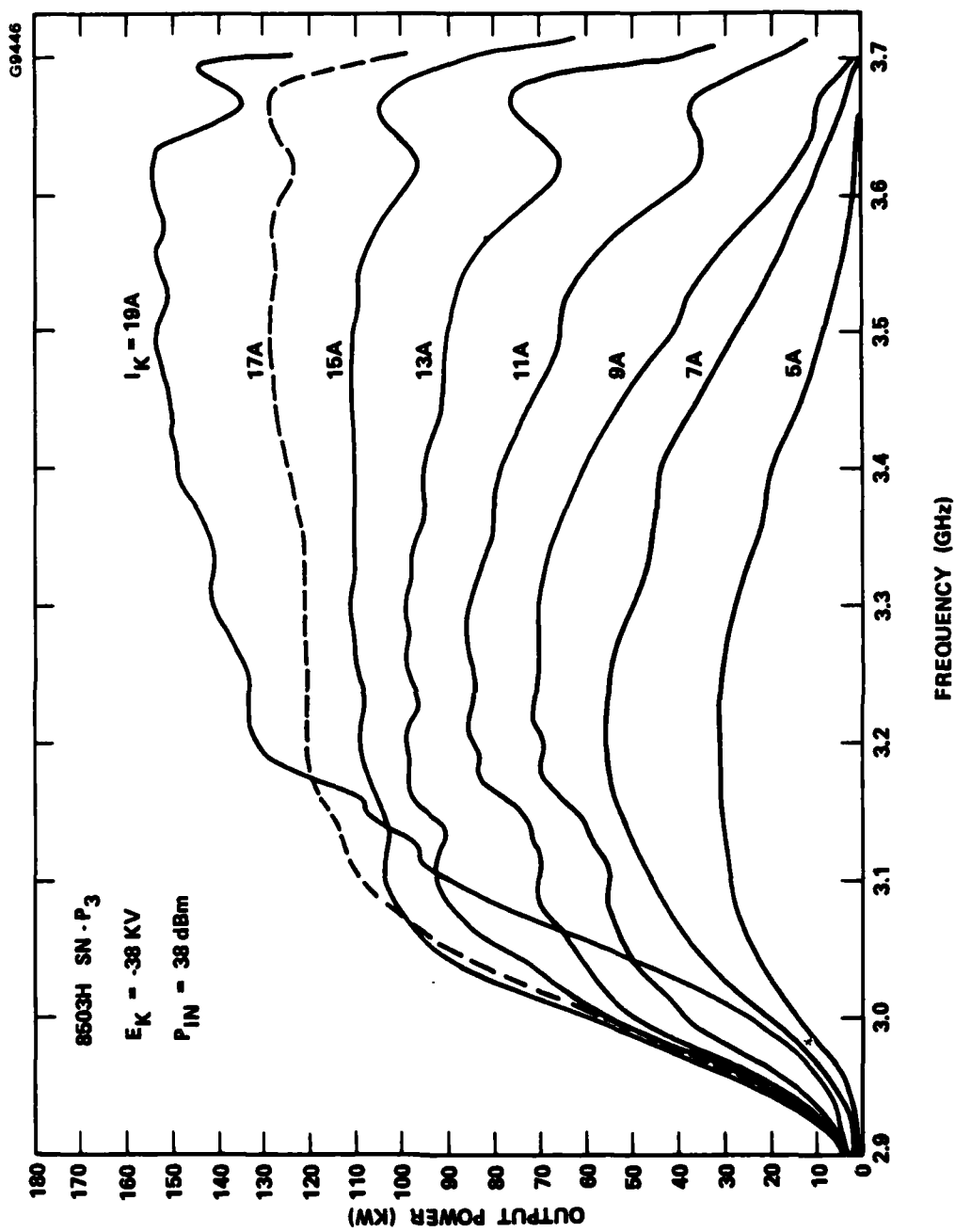


Figure 19 8503H, SN-P<sub>3</sub>, output power vs frequency at a cathode voltage of -38 KV with a constant RF input power of 38 dBm for various values of cathode current.

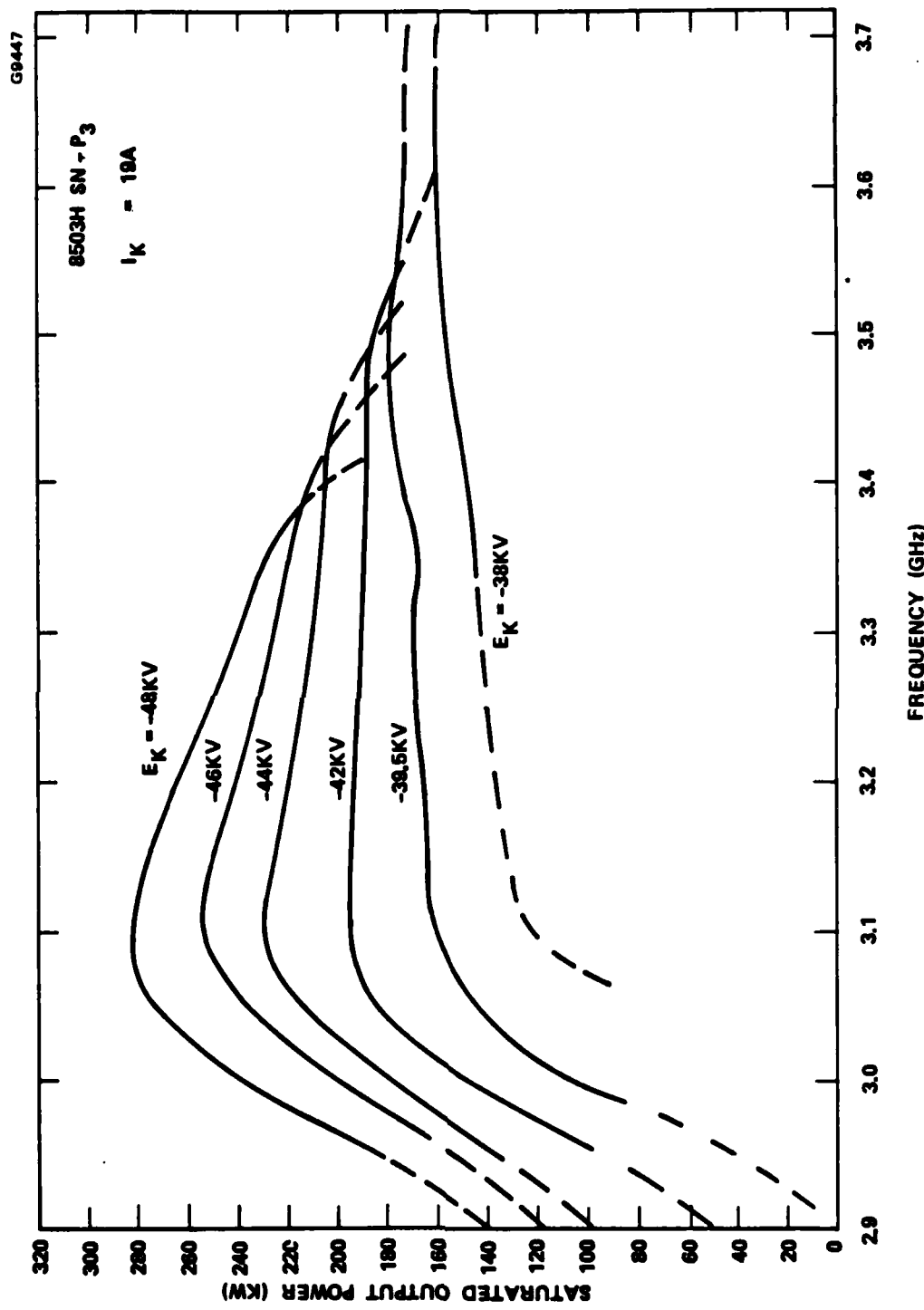


Figure 20 8503H, SN-P<sub>3</sub>, saturated output power vs frequency for various values of cathode voltage with a constant cathode current of 19 amperes.

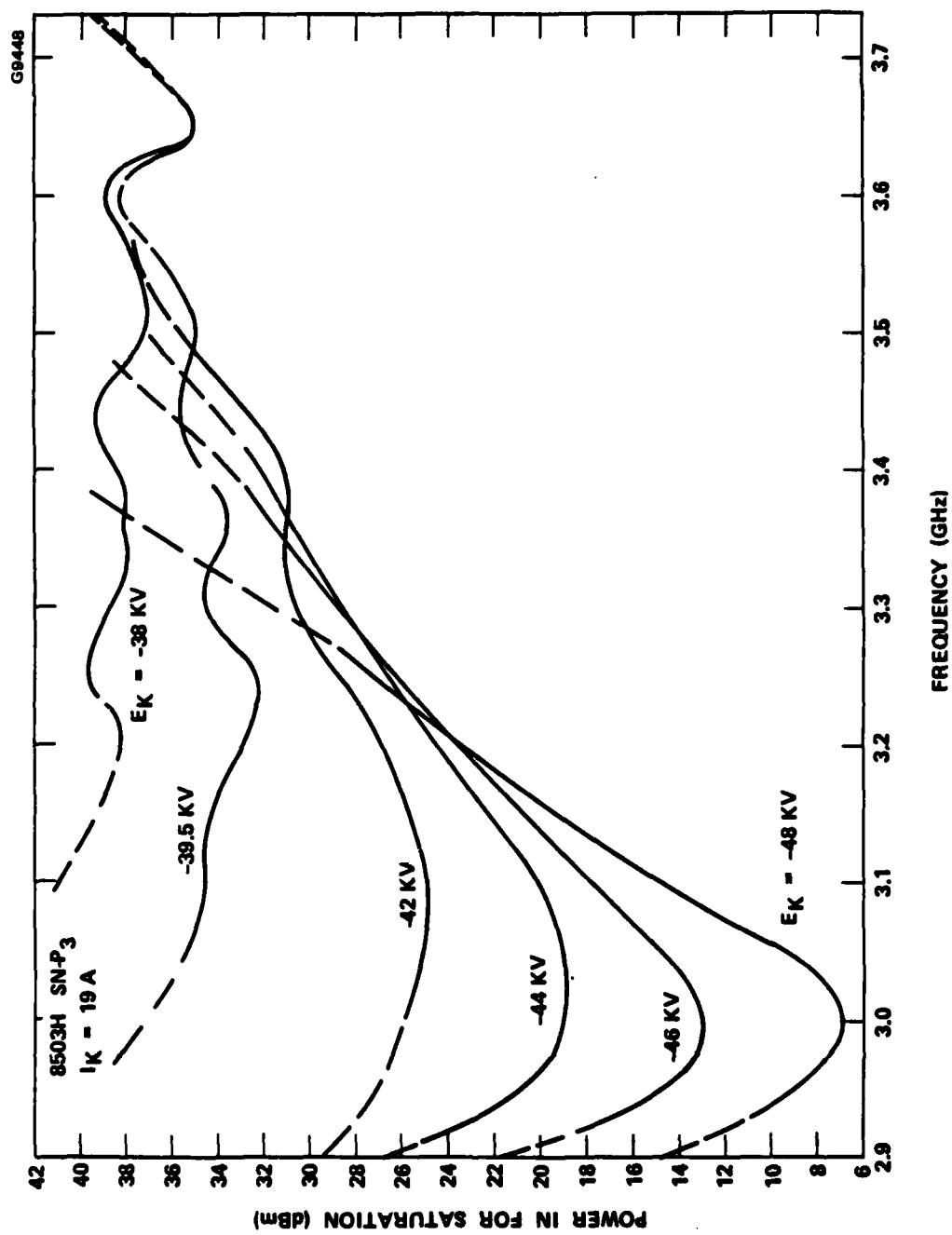


Figure 21 8503H, SN-P3, RF input power required for saturation vs frequency for various values of cathode voltage at a constant cathode current of 19 amperes.

## 5.0 DESIGN ANALYSIS AND DUAL MODE PERFORMANCE

The design of the dual mode TWT was closely guided by the design and performance of the 8503H. Because the 8503H could be operated over a wide range of beam voltages and currents in a satisfactory manner, all major areas of uncertainty that existed at the beginning of the program were resolved. The testing of the 8503H helped in the following areas:

1. Gun performance and beam focusing was demonstrated to be adequate over a large range of gun operating parameters even without changing the focusing field.
2. Tube stability was verified over the same range of gun parameters.
3. Computer predictions of tube performance agreed very well with the measured data. This not only enhanced the confidence in the calculated performance of the dual mode tube, but also established that the beam size corresponded to the expected value (the effective beam filling factor ranged from .70 to .75 with a cathode immersion of 75 percent).

Figure 22 displays the measured and calculated small signal gain versus frequency for three different operating conditions of the 8503H. The measured curves are labeled with the values of the cathode voltage, current, and beam perveance. In the calculations of the small signal gain, the cathode current was reduced by the DC interception on the circuit, while the cathode voltage was adjusted for best overall agreement. The voltage adjustment increased with perveance, ranging from -1.4 percent to -5.8 percent. This kind of adjustment must often be made when using the coupled-cavity computer programs which are based on simple one-dimensional beam models. When done consistently, the results have been excellent. The comparison at large signal levels is shown in Figure 23; the measured data in this case were taken on serial number P2, whereas all other performance data on 8503H presented in this report were taken on P3 which was rather exhaustively evaluated.

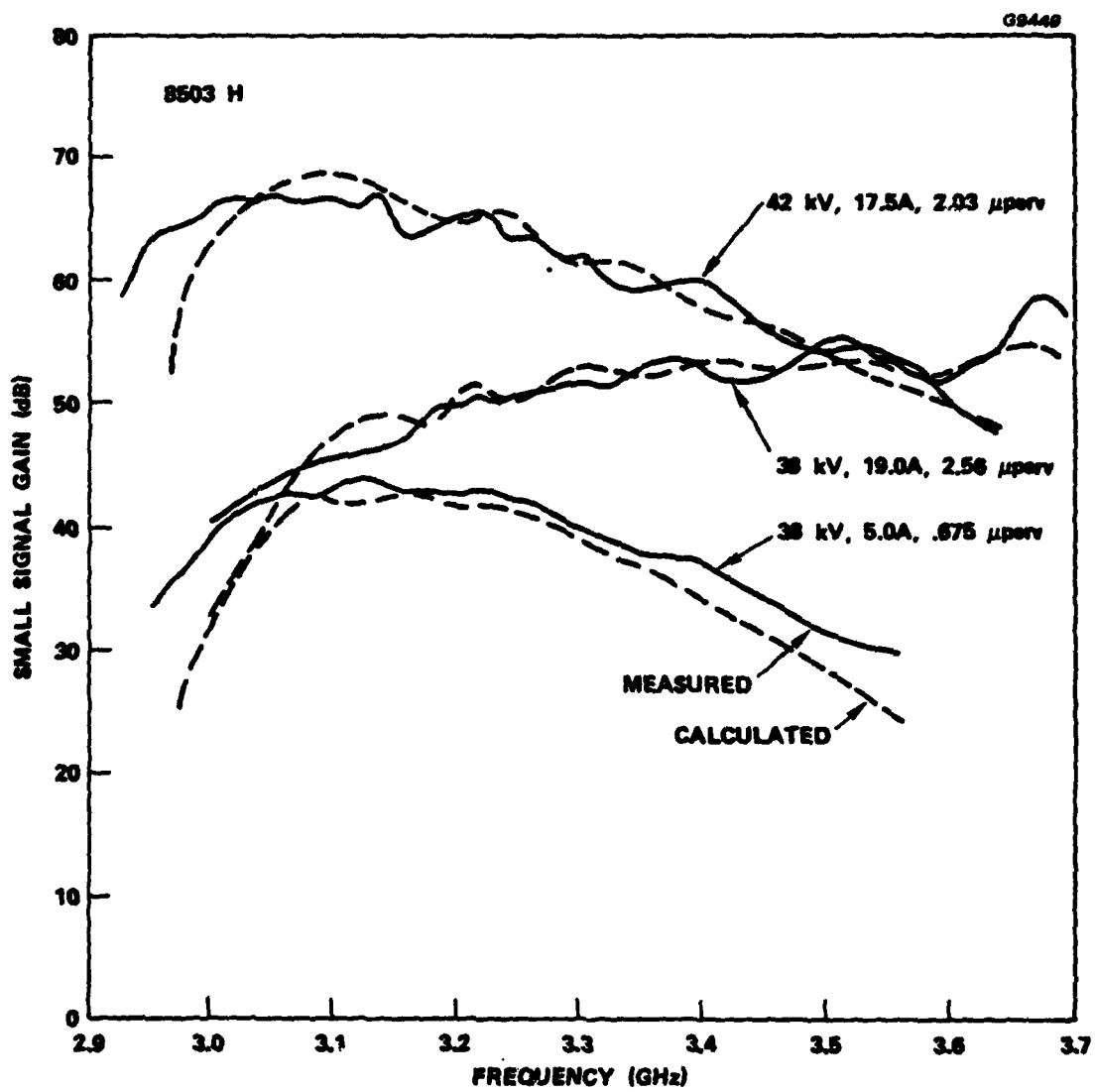


Figure 22 Measured and calculated small signal gain vs frequency of the 8503H at three operating conditions.

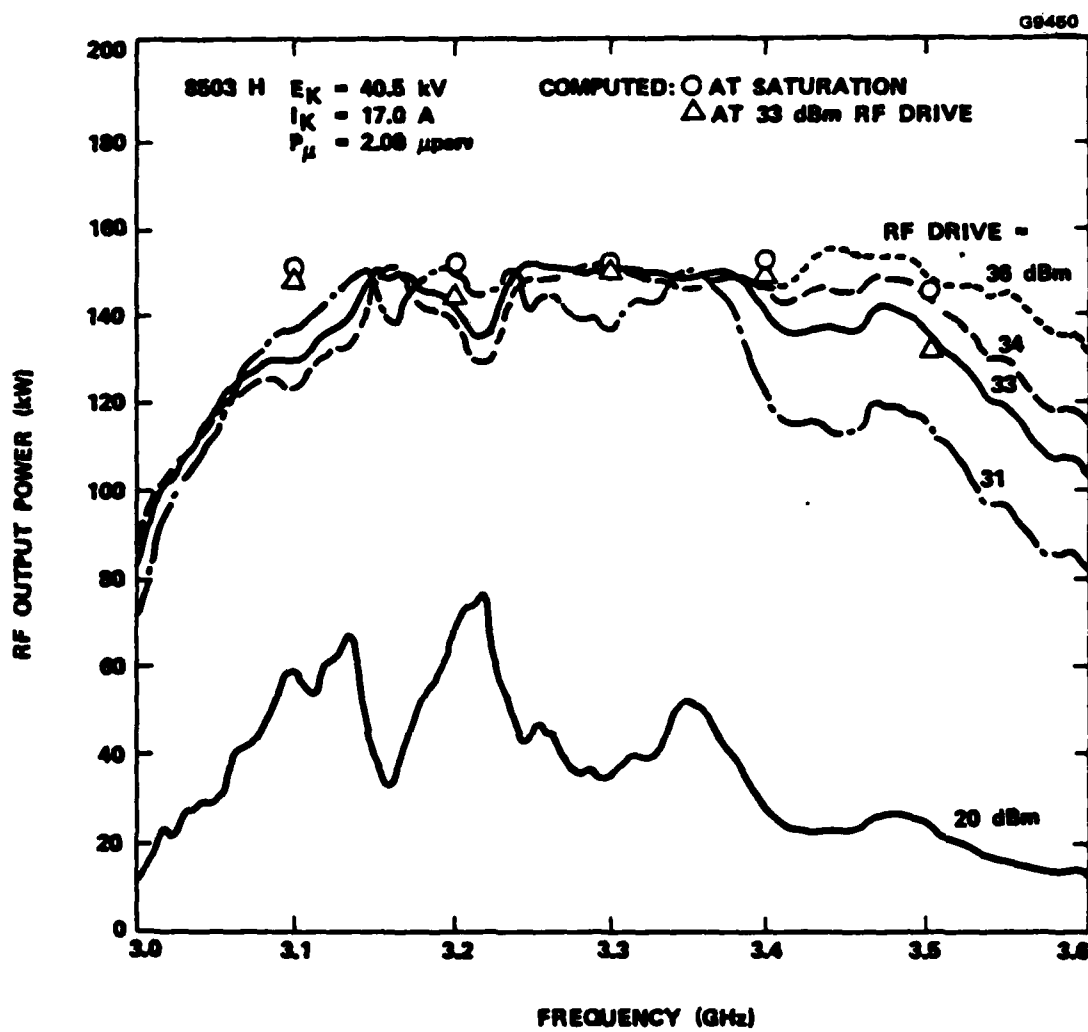


Figure 23   Measured and calculated large signal performance of the 8503H.

Having established that the correlation between the measured and calculated data was good, a circuit for the dual mode TWT was then designed using the 8503H circuit as a general guide. Both circuits include a velocity taper. The circuit length was adjusted to give the same small signal gain at 61.5 kV as the 8503H would have at 41.8 kV, assuming a perveance of about 2.3 in both cases (Figure 24). The voltages refer to actual operating voltages (the values used in the computations being 5 percent lower), while a 96 percent beam transmission was postulated in both cases. By also making the output section gain equal in the two designs, a similar degree of stability can be expected in both devices.

With a circuit design established, the large signal performance was then calculated for several combinations of beam parameters, with the objective of achieving the desired output power performance in the two modes. A satisfactory low mode performance is shown in Figure 25, while Figures 26 and 27 give high mode data. In all cases a beam transmission of 96 percent was assumed. The specified voltages are the actual expected operating values: 54 kV in the low mode providing 110 kW over the 500 MHz at a minimum basic efficiency of 14.5 percent, and 61-62 kV in the high mode giving 500 kW over a 400 MHz band (with constant drive) at 21-22 percent minimum efficiency. The required drive level has to be increased from 35 dBm in the high mode to 45 dBm in the low mode. The small signal gain and saturated gain in both modes are plotted in Figure 28.

The large signal calculations also provide information on the spent beam energy distribution, which determines collector performance. The results show that a single stage collector could be depressed to 40 percent in the low mode and to 25 percent in the high mode. Assuming 90 percent beam collection, that would result in an overall efficiency of 21-27 percent over the band in the low mode and 27-32 percent in the high mode.

A rather promising design for the dual mode TWT has been established, although it has the drawback of requiring a change in cathode voltage between the two modes. Because its essential elements are supported by experimental data, it is felt that a great deal of confidence can be placed on the predicted performance.

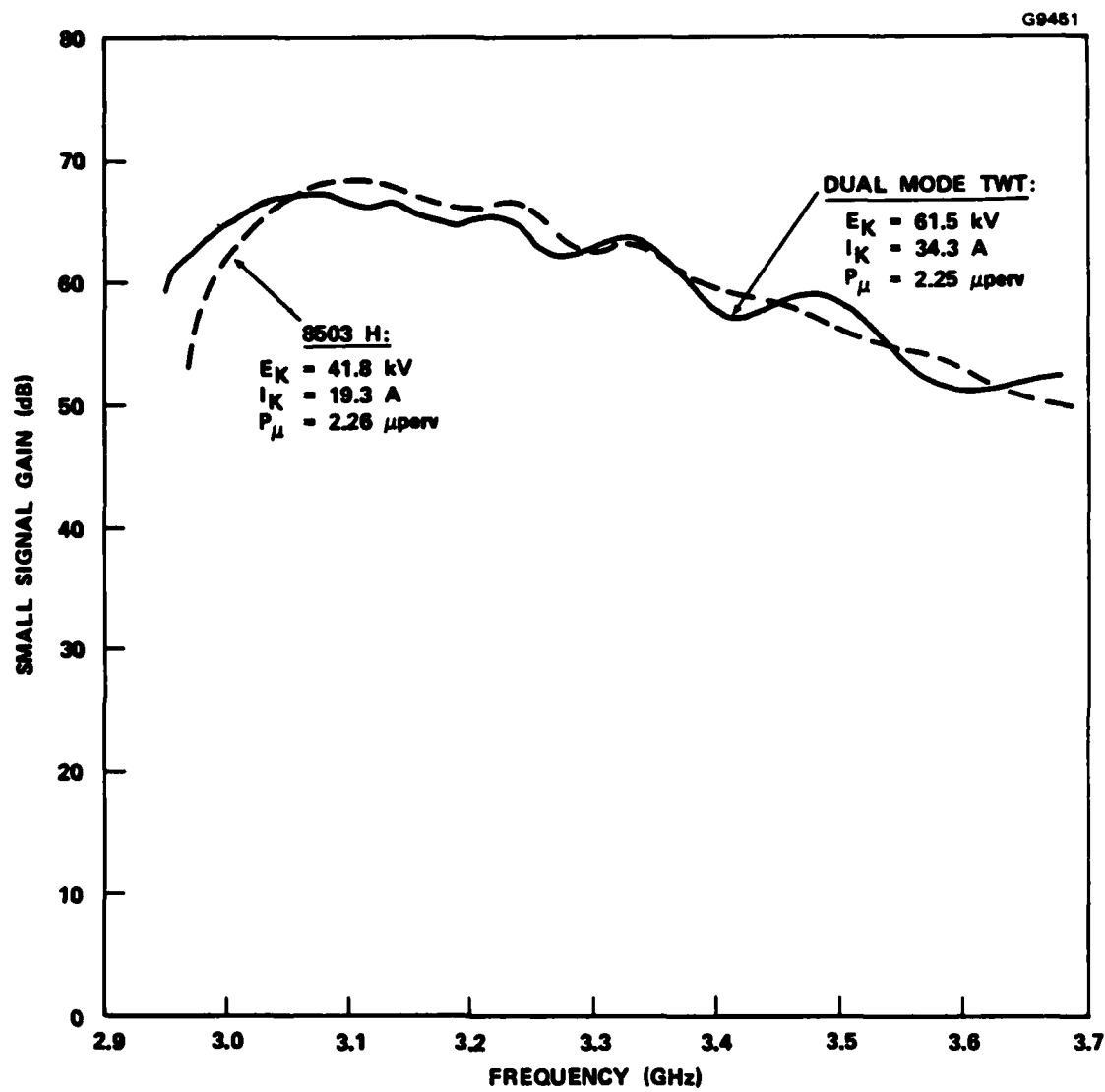


Figure 24 Commonality of small signal gain for the 8503H and the dual mode TWT circuits.

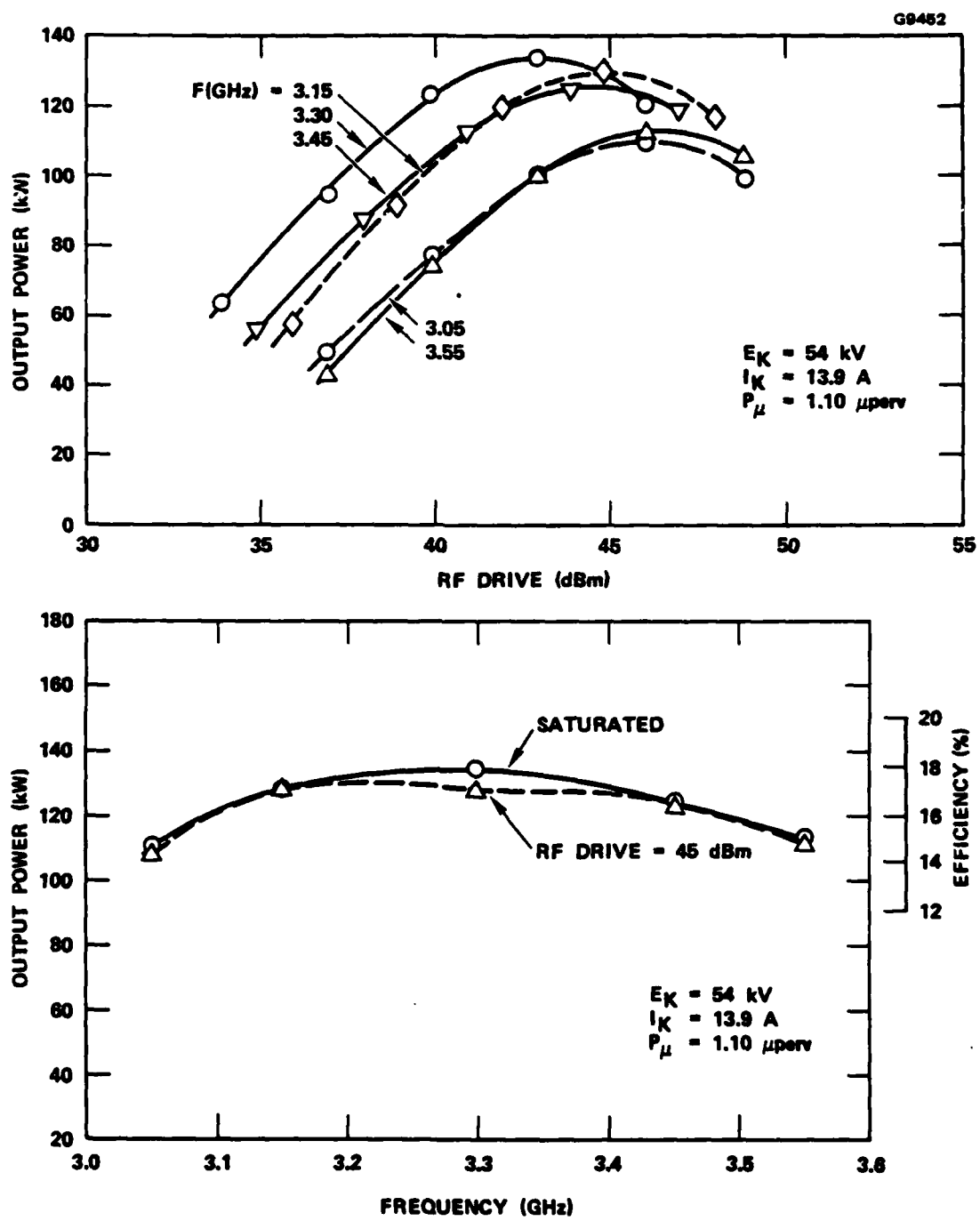


Figure 25 Large signal performance of the dual mode TWT in the low power mode at 54 kV cathode voltage.

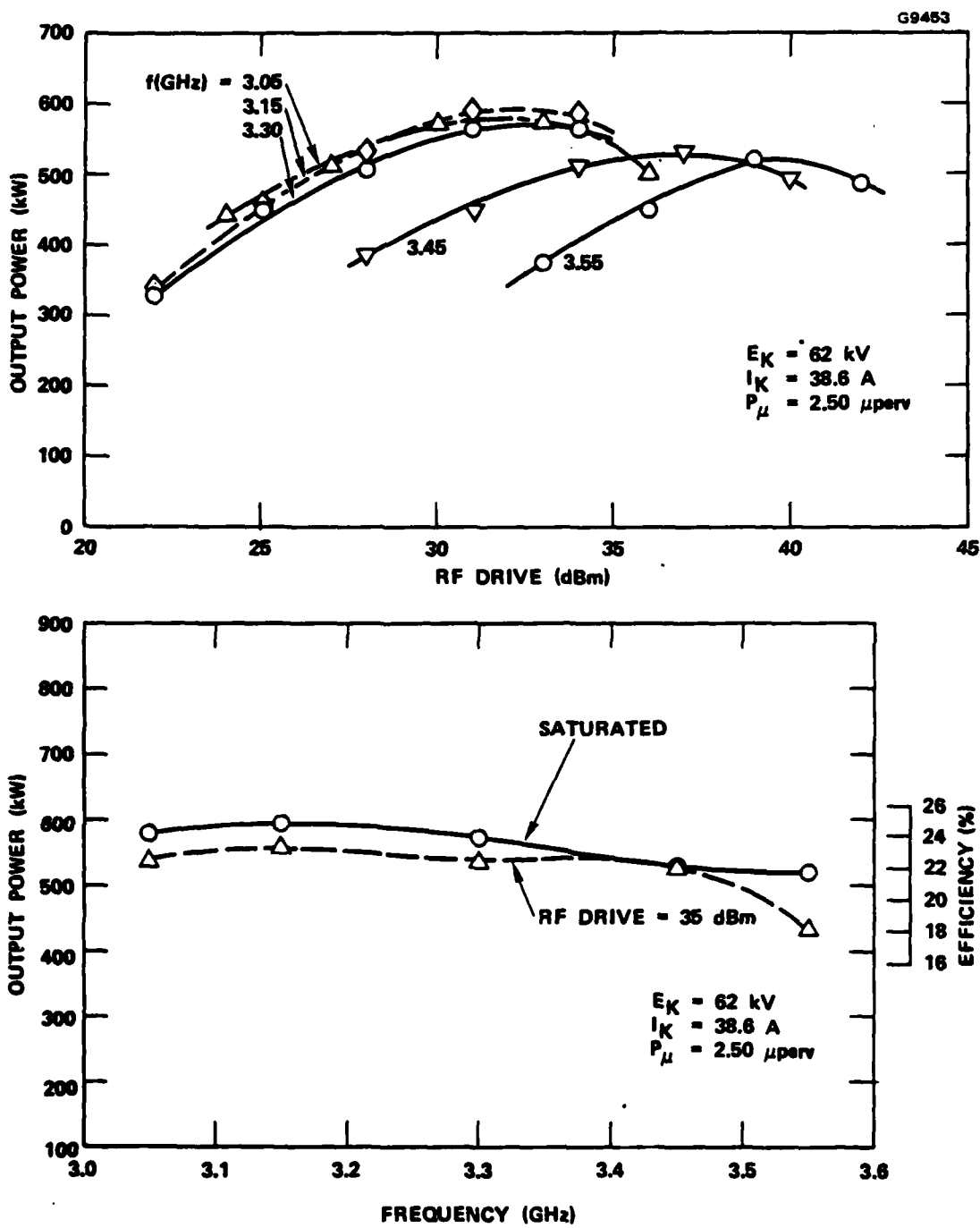


Figure 26 Large signal performance of the dual mode TWT in the high power mode at 62 kV cathode voltage.

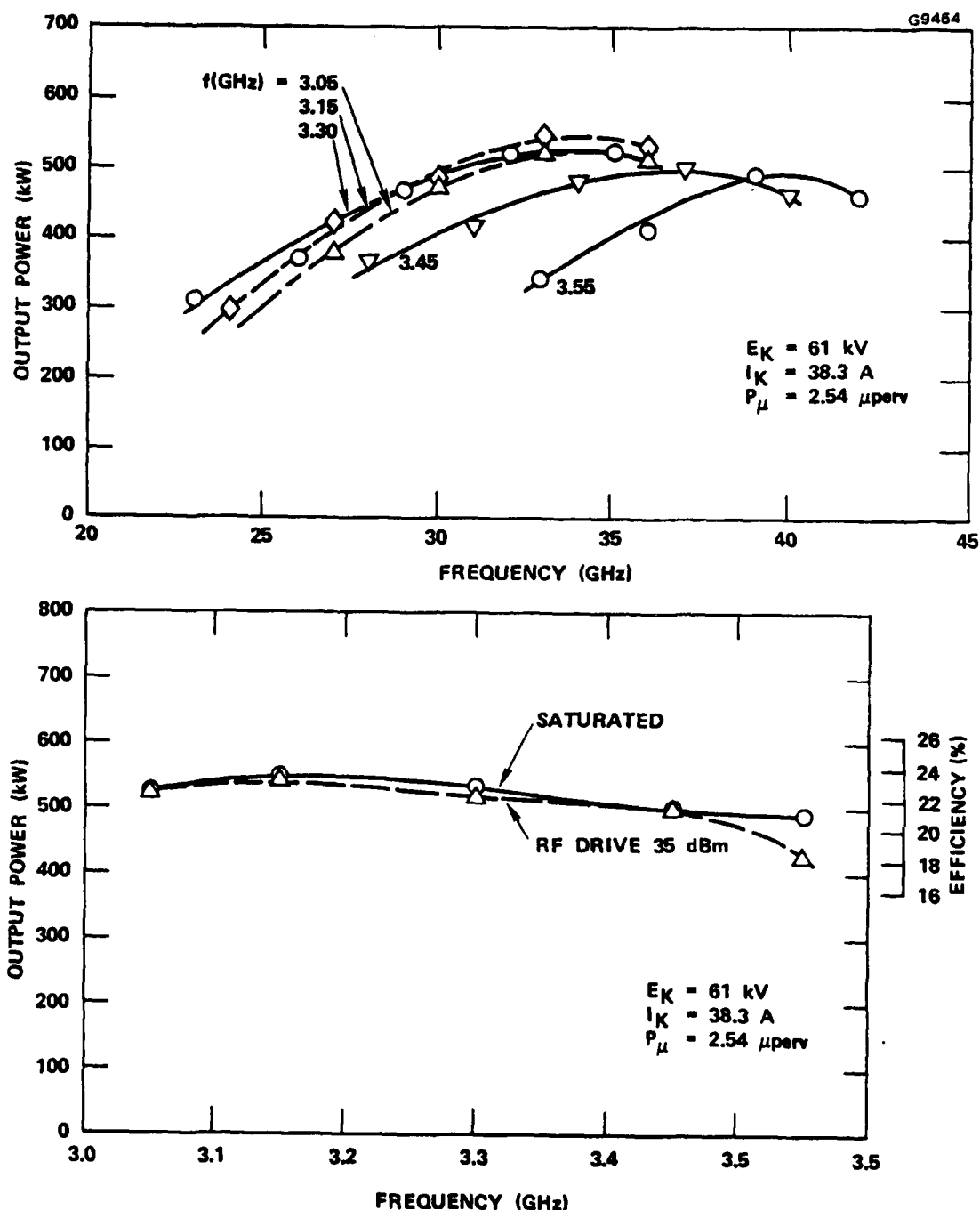


Figure 27 Large signal performance of the dual mode TWT in the high power mode at 61 kV cathode voltage.

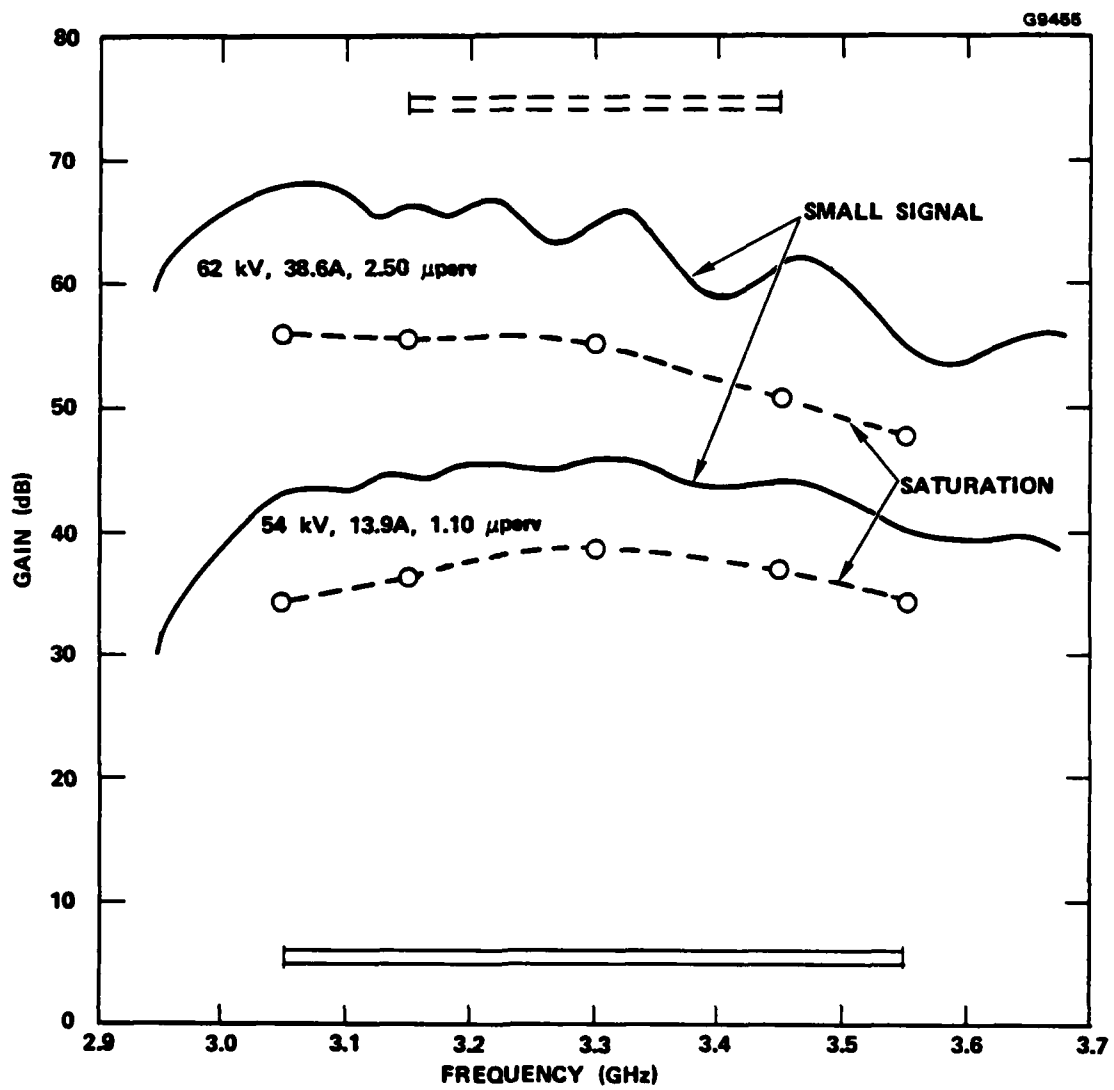


Figure 28 Small signal and saturated g. in vs frequency of the dual mode TWT in both modes.

## 6.0 CONCLUSIONS AND RECOMMENDATIONS

The Multimode Amplifier Program has indicated that the requirement for a single amplifier operating at two distinctly different power levels of 100 kW peak over a 500 MHz bandwidth at S-Band can be satisfied with a coupled-cavity traveling-wave tube using a standard "shadow-grid" electron gun. Good beam transmission at the two operating levels can be maintained by the use of an axial magnetic field, provided by a solenoid, in which a portion of the magnetic field lines thread the cathode emitting surface. This conclusion is based on theoretical calculations which are derived from actual operating data obtained on 8503H traveling-wave tubes.

In switching between the two modes, the RF input power level must be changed and the DC cathode voltage and grid pulse voltage must be set to different levels. With these adjustments, fairly flat gain versus frequency responses can be obtained. Under these conditions, programming the RF input drive versus frequency would not be necessary to cover the required bandwidth.

The data from the 8503H tubes have also suggested that significant dual mode performance could be obtained by merely adjusting the grid voltage and RF input power, keeping the cathode voltage constant. The bandwidth would be more restricted and the gain versus frequency response at the two modes would not be flat as when the cathode voltage is also adjusted.

In order to determine whether such a dual mode traveling-wave tube would be useful in an actual system application, the feasibility of providing the voltage and RF drive adjustments that are necessary when switching between modes would have to be evaluated. If a practical modulator can be provided to supply these adjustments in a manner that would be consistent with the other system requirements, then it would be recommended that a tube that has been designed to the proper parameters as determined in the present program should be fabricated and tested to verify the theoretical conclusions.

**MISSION**  
of  
*Rome Air Development Center*

RADC plans and executes research, development, test and selected acquisition programs in support of Command, Control, Communications and Intelligence (C3I) systems. Technical and engineering support of the Army's space and communications is provided to the Strategic Defense (SD) and Space Defense elements. The primary technical mission is to support communications, electronic warfare, intelligence, space surveillance, space and command control, space-based sensor collection and mobility, space-based strategic and theater ionospheric management, space-based environmental monitoring, physics and electronic resources, and space-based survivability.